Supplementary Information (SI) for Chemical Communications.

Electronic Supplementary Information

Urea-fused and π-extended single-benzene fluorophores with ultralarge Stokes shifts

Taehyeon Choi$^+$, Heechan Kim$^+$, Younghun Kim$^+$, and Dongwhan Lee*

Department of Chemistry, Seoul National University, 1 Gwanak-ro, Gwanak-gu, Seoul 08826, Korea
$^+$These authors contributed equally to this work.

Experimental Section

General Considerations. All reagents were purchased from commercial suppliers and used as received unless otherwise noted. All air-sensitive manipulations were carried out under inert atmosphere by Schlenk-line techniques. All microwave-assisted synthesis was performed in a Biotage® Initiator+ microwave synthesizer. Spectroscopic grade dichloromethane, cyclohexane, toluene, EtOAc, and MeOH were used for solvent-dependent photophysical measurements. All air-sensitive manipulations were carried out under argon atmosphere by standard Schlenk-line techniques. The compounds 1,1'-(2,3-diamino-1,4-phenylene)bis(ethan-1-one) (*o*-**DAPA**),[1] 3,6-di(pyridin-2-yl)benzene-1,2-diamine,[2] 2,1,3-benzothiadiazole-4,7-bis(boronic acid pinacol ester) (**1**),[3] and 4-(4,4,5,5-tetramethyl-1,3,2-dioxaborolan-2-yl)benzo[*c*][1,2,5]thiadiazole (**5**)[4] were prepared according to the reported procedures.

Physical Measurements. ^{1}H NMR and ^{13}C NMR spectra were recorded on a 400 MHz Agilent 400-MR DD2 Magnetic Resonance System and a 500 MHz Varian/Oxford As-500 spectrometer. Chemical shifts were referenced to the residual solvent peaks for ^{1}H NMR and ^{13}C NMR spectra. FT-IR spectra were recorded on a PerkinElmer Spectrum Two FT-IR Spectrophotometer. High-resolution electrospray ionization (ESI) mass spectra were obtained on a Thermo Scientific LTQ Orbitrap XL mass spectrometer. UV–vis spectra were recorded on an Agilent 8453 UV–vis spectrophotometer with ChemStation software. Fluorescence spectra were recorded on a Photon Technology International Quanta-Master 400 spectrofluorometer with FelixGX software. Quantum yields were determined by using a 3.2-inch K-Sphere Petite integrating sphere attached to the spectrofluorometer. Single-crystal X-ray diffraction (SC-XRD) studies were carried out using Cu Kα radiation on an XtaLAB AFC12 (RINC): Kappa dual home/near diffractometer.

---

[1] H. Kim, W. Park, Y. Kim, M. Filatov, C. H. Choi, and D. Lee, *Nat. Commun.*, 2021, **62**, 5409.

[2] I. Pochorovski, J. Milić, D. Kolarski, C. Gropp, W. B. Schweizer and F. Diederich, *J. Am. Chem. Soc.*, 2014, **136**, 3852–3858.

[3] H. Wang, G. Zhou, H. Gai and X. Chen, *Chem. Commun.*, 2012, **48**, 8341–8343.

[4] Z. Ni, H. Wang, H. Dong, Y. Dang, Q. Zhao, X. Zhang and W. Hu, *Nat. Chem.*, 2019, **11**, 271–277.

Computational Studies. All density functional theory (DFT) and time-dependent density functional theory (TD-DFT) calculations were performed with Gaussian 16 program suite.[5] Ground-state and excited-state geometry optimizations were carried out with DFT and TD-DFT calculations using B3LYP hybrid functional with Grimme's D3 dispersion correction[6] (B3LYP-D3) and 6-31++G(d,p) basis set. Vibrational frequency calculations were performed to confirm that all optimized geometries converged to minima or saddle points for transition states. Zero-point and thermal corrections were made to the electronic energies to obtain Gibbs free energies of the optimized geometries. Solvation was considered by self-consistent reaction field (SCRF) calculations with conductor-like polarizable continuum model (CPCM) of CH_2Cl_2 ($\varepsilon = 8.93$).[7] The S_1 potential energy curves of **BZ-1**, **BZ-2**, and **BZ-3′** (Fig. S1) are constructed by a relax scan along the fixed $NH\cdots X_{acceptor}$ distance (29 points; step = 0.05 Å). The 2D S_1 potential energy surface of **BZ-3′** (Fig. 3b) was constructed by a relax scan along the fixed $N1\cdots H1$ and $N1'\cdots H1'$ distances (196 points; step = 0.1 Å). The minimum energy path of the ESIPT reaction (Fig. 3b, white line) was constructed by a relaxed scan of geometries with fixed $N1\cdots H1$ distance (from $S_{1,N*}$ to $S_{1,T*}$) and fixed $N1'\cdots H1'$ distance (from $S_{1,T*}$ to $S_{1,TT*}$) generated by linear interpolation between the stationary points. The proton transfer reaction coordinate (Fig. 3c) is represented by a cumulative distance of the minimum energy path (Fig. 3b, white line) starting from S_1 FC. The S_1 potential energy curve of protonated **BZ-3′** (Fig. S7) is constructed by a relax scan along the fixed C7–C6–C5–N1 dihedral angle (step = 20°) (9 points; step = 20°).

---

[5] M. J. Frisch, G. W. Trucks, H. B. Schlegel, G. E. Scuseria, M. A. Robb, J. R. Cheeseman, G. Scalmani, V. Barone, G. A. Petersson, H. Nakatsuji, X. Li, M. Caricato, A. V. Marenich, J. Bloino, B. G. Janesko, R. Gomperts, B. Mennucci, H. P. Hratchian, J. V. Ortiz, A. F. Izmaylov, J. L. Sonnenberg, D. Williams-Young, F. Ding, F. Lipparini, F. Egidi, J. Goings, B. Peng, A. Petrone, T. Henderson, D. Ranasinghe, V. G. Zakrzewski, J. Gao, N. Rega, G. Zheng, W. Liang, M. Hada, M. Ehara, K. Toyota, R. Fukuda, J. Hasegawa, M. Ishida, T. Nakajima, Y. Honda, O. Kitao, H. Nakai, T. Vreven, K. Throssell, J. A. Montgomery, Jr., J. E. Peralta, F. Ogliaro, M. J. Bearpark, J. J. Heyd, E. N. Brothers, K. N. Kudin, V. N. Staroverov, T. A. Keith, R. Kobayashi, J. Normand, K. Raghavachari, A. P. Rendell, J. C. Burant, S. S. Iyengar, J. Tomasi, M. Cossi, J. M. Millam, M. Klene, C. Adamo, R. Cammi, J. W. Ochterski, R. L. Martin, K. Morokuma, O. Farkas, J. B. Foresman, and D. J. Fox, Gaussian 16 (Revision B.01), Gaussian Inc., Wallingford, CT, 2016.

[6] S. Grimme, J. Antony, S. Ehrlich, and H. Krieg, *J. Chem. Phys.*, 2010, **132**, 154104.

[7] J. Tomasi, B. Mennucci, and R. Cammi, *Chem. Rev.*, 2005, **105**, 2999–3094.

Scheme S1. Synthetic route to **BZ-1**.

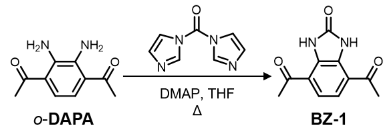

***o*-DAPA**

BZ-1

1,1'-(2-Oxo-2,3-dihydro-1*H*-benzo[*d*]imidazole-4,7-diyl)bis(ethan-1-one) (BZ-1). A 50 mL round-bottom was charged with 1,1'-(2,3-diamino-1,4-phenylene)bis(ethan-1-one) (*o*-**DAPA**) (91.1 mg, 0.474 mmol), 4-dimethylaminopyridine (10 mg, 0.081 mmol), 1,1'-carbonyldiimidazole (174 mg, 1.07 mmol), and THF (8 mL). The mixture was heated at reflux for 1 d. After cooling to r.t., the precipitate was gathered by filtration to furnish **BZ-1** as a yellow solid (25.0 mg, 0.115 mmol, yield = 24%). ^{1}H NMR (500 MHz, DMSO-d_6, 298 K): δ 10.95 (s, 2H), 7.65 (s, 2H), 2.63 (s, 6H). ^{13}C NMR (100 MHz, DMSO-d_6, 298 K): δ 198.42, 156.26, 130.69, 121.65, 120.87, 28.02. FT-IR(ATR, cm^{-1}): 3744, 3711, 3629, 3312, 3192, 3006, 2988, 2923, 2851, 2650, 2374, 2337, 2325, 2287, 2186, 2163, 2051, 2020, 1981, 1966, 1711, 1665, 1597, 1497, 1462, 1370, 1319, 1276, 1259, 1221, 1200, 1143, 992. HRMS (ESI) calcd for $C_{11}H_{11}N_2O_3$ [M+H]$^+$ 219.0764, found 219.0767.

Scheme S2. Synthetic route to **BZ-2**.

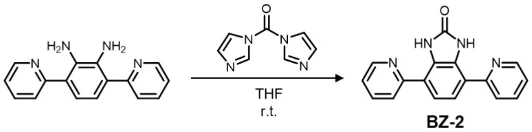

BZ-2

4,7-Di(pyridin-2-yl)-1,3-dihydro-2*H*-benzo[*d*]imidazol-2-one (BZ-2). A 20 mL vial was charged with 3,6-di(pyridin-2-yl)benzene-1,2-diamine (0.128 g, 0.381 mmol), 1,1'-carbonyldiimidazole (98.0 mg, 0.762 mmol), and THF (4 mL). The reaction mixture was stirred at r.t. for 1 d, diluted with MTBE (100 mL) and the precipitate was isolated by filtration to furnish **BZ-2** as a white solid (91.1 mg, 0.316 mmol, yield = 83%). ^{1}H NMR (500 MHz, CD_2Cl_2, 298 K): δ 10.38 (s, 2H), 8.70 (ddd, J = 4.9, 1.9, 1.0 Hz, 2H), 7.99 (dt, J = 8.1, 1.1 Hz, 2H), 7.85 (td, J = 7.8, 1.9 Hz, 2H), 7.67 (s, 2H), 7.27 (ddd, J = 7.4, 4.8, 1.1 Hz, 2H). ^{13}C NMR (125 MHz, CD_2Cl_2, 298 K): δ 155.66, 154.59, 148.98, 136.95, 129.56, 122.03, 119.78, 119.20, 117.99. FT-IR(ATR, cm^{-1}): 3745, 3363, 3218, 3060, 3012, 2920, 2851, 2325, 2187, 2163, 2139, 2115, 2087, 2051, 1980, 1967, 1868, 1782, 1686, 1620, 1609, 1586, 1566, 1518, 1473, 1457, 1432, 1415, 1384, 1358, 1321, 1303, 1272, 1253, 1211, 1180, 1160, 1129, 1088, 1049, 988, 981, 936, 913, 893, 877. HRMS (ESI) calcd for $C_{17}H_{12}N_4O$ [M+H]$^+$ 289.1084, found 289.1085.

Scheme S3. Synthetic route to **BZ-3**.

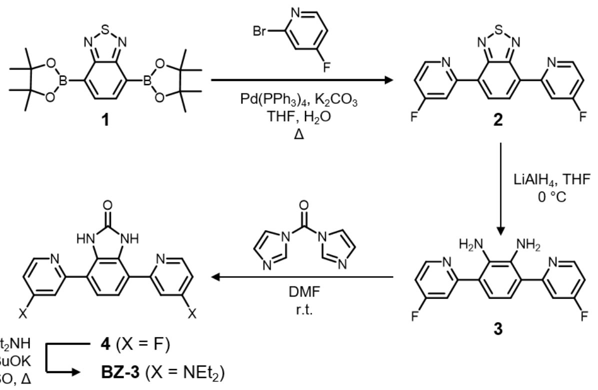

4,7-Bis(4-fluoropyridin-2-yl)benzo[*c*][1,2,5]thiadiazole (2). A 250 mL 3-neck round-bottom flask was charged with benzothiadiazole-4,7-bis(boronic acid pinacol ester) (**1**) (1.00 g, 2.58 mmol), $Pd(PPh_3)_4$ (0.145 g, 0.129 mmol), K_2CO_3 (1.75 g, 12.7 mmol), water (5 mL) and dry THF (50 mL) under an argon atmosphere. A portion of 2-bromo-4-fluoropyridine (0.56 mL, 5.4 mmol) was added and the solution was stirred at 80 °C for 19 h. The reaction mixture was poured into water (100 mL), and extracted into CH_2Cl_2 (100 mL × 3). The combined organic layer was dried over anhyd Na_2SO_4, filtered, and concentrated under reduced pressure. Flash column chromatography on SiO_2 (hexane:EtOAc = 2:1 to 1:1, v/v) furnished **2** as a yellow solid (0.544 g, 1.67 mmol, yield = 65%). ^{1}H NMR (400 MHz, $CDCl_3$, 298 K): δ 8.80 – 8.70 (m, 4H), 8.70 – 8.62 (m, 2H), 7.11 (dddd,J = 8.0, 5.5, 2.4, 1.1 Hz, 2H). ^{13}C NMR (125 MHz, CD_2Cl_2, 298 K): δ 170.65, 168.58, 156.94, 156.87, 154.05, 152.40, 152.35, 130.26, 113.60, 113.44, 111.40, 111.27. FT-IR(ATR, cm^{-1}): 3711, 3103, 3072, 3006, 2988, 2924, 2853, 2650, 2317, 2287, 2186, 2163, 2141, 2051, 2012, 1982, 1716, 1670, 1591, 1576, 1565, 1543, 1462, 1417, 1374, 1345, 1295, 1275, 1261, 1211, 1169, 1113, 1081, 1006, 972, 867, 840, 824. HRMS (ESI) calcd for $C_{16}H_8F_2N_4S$ $[M+H]^+$ 327.0510, found 327.0515.

3,6-Bis(4-fluoropyridin-2-yl)benzene-1,2-diamine (3). An oven-dried 100 mL 2-neck round-bottom flask was charged with **2** (0.963 g, 2.95 mmol) and dry THF (100 mL) under an argon atmosphere. The solution was stirred at 0 °C, and dry $LiAlH_4$ (2 M in THF solution), (10 mL) was added dropwise over a period of 5 min. The reaction mixture was stirred at r.t. for 1 h and quenched with water (10 mL) at 0 °C. The mixture was poured CH_2Cl_2 (200 mL), dried over anhyd Na_2SO_4, filtered, and concentrated under reduced pressure. Flash column chromatography on SiO_2 (hexane:EtOAc = 100:0 to 50:50, v/v) furnished **3** as an orange solid (0.472 g, 1.58 mmol, yield = 54%). ^{1}H NMR (500 MHz, $CDCl_3$, 298 K): δ 8.63 (dd, J = 9.0, 5.7 Hz, 2H), 7.46 (dd, J = 10.9, 2.4 Hz, 2H), 7.12 (d,J = 1.0 Hz, 2H), 6.97 (ddd, J = 8.3, 5.7, 2.4 Hz, 2H), 5.70 (s, 4H). ^{13}C NMR (125 MHz, $CDCl_3$, 298 K): δ 170.47, 168.39, 162.57, 162.51, 150.57, 150.51, 137.13, 122.21, 122.18, 118.78, 110.06, 109.93, 109.50, 109.36. FT-IR (ATR, cm^{-1}): 3745, 3647, 3104, 3072, 2924, 2853, 2347, 2325, 2286, 2187, 2163, 2140, 2116, 2074, 2051, 1982, 1600, 1591, 1576, 1565, 1543, 1494, 1462, 1417, 1345, 1295, 1274, 1263, 1211, 1169, 1113, 1081, 1006, 972, 867, 840, 824. HRMS (ESI) calcd for $C_{16}H_{12}F_2N_4$ $[M+H]^+$ 299.1103, found 299.1105.

4,7-Bis(4-fluoropyridin-2-yl)-1,3-dihydro-2*H*-benzo[d]imidazol-2-one (4). A 250 mL round-bottom flask was charged with **3** (95.0 mg, 0.318 mmol), 1,1'-carbonyldiimidazole (155 mg, 0.956 mmol), and DMF (3 mL). The reaction mixture was stirred at r.t. for 1 d, diluted with MTBE (60 mL), and the precipitate was isolated by filtration to furnish **4** as a white solid (73.0 mg, 0.225

mmol, yield = 71%). ^{1}H NMR (500 MHz, $CDCl_3$, 298 K): δ 10.39 (s, 2H), 8.66 (dd, J = 8.7, 5.6 Hz, 2H), 7.65 (dd, J = 10.5, 2.3 Hz, 2H), 7.57 (s, 2H), 7.02 (ddd, J = 8.0, 5.6, 2.3 Hz, 2H). ^{13}C NMR (125 MHz, DMSO-d_6, 298 K): δ 170.47, 168.42, 158.61, 158.55, 155.22, 152.62, 152.56, 129.58, 119.57, 119.54, 119.49, 110.67, 110.53, 108.70, 108.56. FT-IR(ATR, cm^{-1}): 3186, 3006, 2971, 2925, 2870, 2852, 2692, 2341, 2325, 2287, 2187, 2163, 2143, 2074, 2051, 2023, 1981, 1701, 1594, 1537, 1508, 1454, 1377, 1357, 1304, 1273, 1255, 1197, 1176, 1159, 1138, 1097, 1079, 1059, 1027, 986, 869, 834, 809. HRMS (ESI) calcd for $C_{17}H_{10}F_2N_4O$ $[M+H]^+$ 325.0895, found 325.0902.

4,7-Bis(4-(diethylamino)pyridin-2-yl)-1,3-dihydro-2*H*-benzo[d]imidazol-2-one (BZ-3). A 10–20 mL Biotage® Microwave Reaction Vial was charged with **4** (49.3 mg, 0.152 mmol), dietylamine (0.5 mL, 10 mmol), TMSCl (0.1 mL, 0.8 mmol), KO_tBu (34.6 mg, 0.308 mmol), and DMSO (5 mL) under a argon sparge. The mixture was heated by microwave irradiation at 100 °C with stirring for 12 h, cooled to r.t., poured into EtOAc (100 mL), and washed with water (75 mL × 3). The organic layer was dried over anhyd Na_2SO_4, filtered, and concentrated under reduced pressure. Flash column chromatography on SiO_2 (CH_2Cl_2:MeOH = 10:0 to 9:1, v/v) furnished **BZ-3** as a white solid (58.3 mg, 0.135 mmol, yield = 89%). ^{1}H NMR (500 MHz, $CDCl_3$, 298 K): δ 10.52 (s, 2H), 8.25 (d, J = 6.0 Hz, 2H), 7.53 (s, 2H), 7.05 (d, J = 2.5 Hz, 2H), 6.45 (dd, J = 6.1, 2.5 Hz, 2H), 3.46 (q, J = 7.2 Hz, 8H), 1.25 (t, J = 7.1 Hz, 12H). ^{13}C NMR (125 MHz, $CDCl_3$, 298 K): δ 156.07, 155.11, 152.85, 149.17, 129.74, 120.22, 117.82, 105.28, 102.14, 44.16, 12.55. FT-IR(ATR, cm^{-1}): 3745, 3243, 3004, 2972, 2931, 2894, 2325, 2193, 2164, 2140, 2116, 2051, 1982, 1967, 1690, 1593, 1538, 1493, 1474, 1425, 1377, 1354, 1308, 1297, 1274, 1260, 1197, 1156, 1137, 1094, 1080, 1028, 988, 913, 836. HRMS (ESI) calcd for $C_{25}H_{30}N_6O$ $[M+H]^+$ 431.2554, found 431.2562.

Scheme S4. Synthetic route to **BZ-4**.

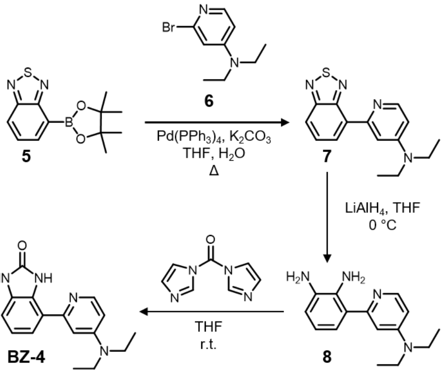

2-Bromo-*N*,*N*-diethylpyridin-4-amine (6). A 250 mL round-bottom flask was charged with 2-bromo-4-fluoropyridine (3.0 mL, 29 mmol), dietylamine (6.0 mL, 58 mmol), K_2CO_3(8.00 g, 57.9 mmol), and DMF (60 mL). The solution was stirred at 65 °C for 1 d, and concentrated under reduced pressure at 70 °C. The reaction mixture was poured into water (100 mL), and extracted into EtOAc (150 mL × 3). The combined organic layer dried over anhyd Na_2SO_4, filtered, and concentrated under reduced pressure. Flash column chromatography on SiO_2 (hexane:EtOAc = 100:0 to 50:50, v/v) furnished **6** as a yellow liquid (6.56 g, 28.7 mmol, yield = 99%).^{1}H NMR (500 MHz, $CDCl_3$, 298 K): δ 7.88 (d, J = 6.1 Hz, 1H), 6.58 (d, J = 2.5 Hz, 1H), 6.38 (dd, J = 6.1, 2.5 Hz, 1H), 3.31 (q, J = 7.1 Hz, 4H), 1.15 (t, J = 7.2 Hz, 6H). ^{13}C NMR (125 MHz, $CDCl_3$, 298 K): δ 153.80, 149.58, 143.45, 108.82, 106.00, 44.17, 12.28. FT-IR(ATR, cm^{-1}): 3728, 3647, 3417, 3172, 3146, 3088, 3037, 2972, 2932, 2899, 2871, 2760, 2664, 2559, 2525, 2504, 2446, 2380, 2363, 2347, 2325, 2275, 2204, 2164, 2144, 2103, 2087, 2051, 2012, 1981, 1904, 1771, 1733, 1661, 1585, 1514, 1503, 1476, 1448, 1401, 1378, 1358, 1307, 1288, 1273, 1252, 1193, 1167, 1129, 1093, 1074, 1015, 974, 923, 808. HRMS (ESI) calcd for $C_9H_{13}BrN_2$ $[M+H]^+$ 229.0335 and 231.0314, found 229.0337 and 231.0314.

2-(Benzo[*c*][1,2,5]thiadiazol-4-yl)-*N*,*N*-diethylpyridin-4-amine (7). A 100 mL 3-neck round-bottom flask was charged with 4-(4,4,5,5-tetramethyl-1,3,2-dioxaborolan-2-yl)benzo[*c*][1,2,5]thiadiazole (**5**) (0.512 g, 1.95 mmol), $Pd(PPh_3)_4$ (0.126 g, 0.109 mmol), K_2CO_3 (1.34 g, 9.70 mmol), **6** (0.509 g, 2.22 mmol), water (5 mL), and dry THF (25 mL) under an argon atmosphere. The solution was stirred at 80 °C for 1 d. The reaction mixture was poured into water (100 mL), and extracted into EtOAc (100 mL × 3). The combined organic layer was dried over anhyd Na_2SO_4, filtered, and concentrated under reduced pressure. Flash column chromatography on SiO_2 (CH_2Cl_2:acetone = 9:1 to 7:3, v/v) furnished **7** as a yellow gummy mareial (0.313 g, 1.10 mmol, yield = 56%).^{1}H NMR (500 MHz, $CDCl_3$, 298 K): δ 8.37 – 8.32 (m, 2H), 8.02 (dd, J = 8.7, 1.2 Hz, 1H), 7.84 (d, J = 2.6 Hz, 1H), 7.71 (dd, J = 8.7, 7.0 Hz, 1H), 6.51 (dd, J = 6.0, 2.7 Hz, 1H), 3.46 (q, J = 7.1 Hz, 4H), 1.25 (t, J = 7.1 Hz, 6H). ^{13}C NMR (125 MHz, $CDCl_3$, 298 K): δ 155.79, 154.29, 153.16, 152.60, 149.85, 133.49, 129.72, 128.93, 121.45, 108.13, 105.52, 105.50, 44.15, 12.46. FT-IR(ATR, cm^{-1}): 3347, 3171, 3133, 3088, 3062, 3039, 2969, 2928, 2895, 2870, 2569, 2513, 2398, 2325, 2292, 2186, 2163, 2115, 2080, 2051, 1981, 1939, 1904, 1840, 1733, 1707, 1668, 1601, 1583, 1539, 1495, 1477, 1447, 1406, 1377, 1357, 1327, 1285, 1265, 1244, 1197, 1156, 1134, 1115, 1095, 1078, 1022, 983, 914, 896, 855, 832, 805. HRMS (ESI) calcd for $C_{15}H_{16}N_4S$ $[M+H]^+$ 285.1168, found 285.1170.

3-(4-(Diethylamino)pyridin-2-yl)benzene-1,2-diamine (8). An 100 mL oven-dried 2-neck round-bottom flask was charged with **7** (0.200 g, 0.703 mmol) and dry THF (20 mL) under an argon atmosphere. The solution was stirred at 0 °C, and dry $LiAlH_4$ (2 M in THF solution), (2.8 mL) was added dropwise over a period of 1 min. The reaction mixture was stirred at r.t. for 1 h and quenched with water (3 mL) at 0 °C. The mixture was poured into CH_2Cl_2 (200 mL), dried over anhyd Na_2SO_4, filtered, and concentrated under reduced pressure. Flash column chromatography on SiO_2 (CH_2Cl_2:MeOH = 100:0 to 9:1, v/v) furnished **8** as a red solid (0.111 g, 0.435 mmol, yield = 62%).^{1}H NMR (400 MHz, $CDCl_3$, 298 K): δ 8.23 (dd, J = 6.1, 1.5 Hz, 1H), 7.01 (dt, J = 6.8, 1.9 Hz, 1H), 6.80 – 6.57 (m, 3H), 6.42 (dd, J = 6.0, 2.5 Hz, 1H), 3.45 – 3.37 (m, 4H), 1.21 (td, J = 7.1, 1.4 Hz, 6H). ^{13}C NMR (125 MHz, $CDCl_3$, 298 K): δ 159.91, 153.08, 148.67, 135.38, 135.31, 126.12, 121.10, 118.42, 116.59, 105.53, 104.60, 44.04, 12.57. FT-IR(ATR, cm^{-1}): 3395, 3329, 3088, 3061, 3029, 2971, 2929, 2894, 2870, 2719, 2522, 2455, 2389, 2325, 2288, 2178, 2163, 2139, 2103, 2087, 2051, 2023, 2009, 1981, 1908, 1731, 1591, 1535, 1502, 1462, 1431, 1395, 1377, 1358, 1293, 1259, 1241, 1196, 1158, 1126, 1094, 1077, 1020, 987, 950, 913, 881, 845. HRMS (ESI) calcd for $C_{15}H_{20}N_4$ $[M+H]^+$ 257.1761, found 257.1763.

2-(Benzo[*c*][1,2,5]thiadiazol-4-yl)-*N*,*N*-diethylpyridin-4-amine (BZ-4). A 20 mL vial was charged with **10** (0.111 g, 0.435 mmol), 1,1'-carbonyldiimidazole (82.9 mg, 0.522 mmol), and DMF (12 mL). The reaction mixture was stirred at r.t. for 1 d, poured into EtOAc (100 mL), and washed with water (75 mL × 3). The organic layer was dried over anhyd Na_2SO_4, filtered, and concentrated under reduced pressure. Flash column chromatography on SiO_2 (CH_2Cl_2:MeOH = 10:0 to 9:1, v/v) furnished **BZ-4** as a yellow solid (87.2 mg, 0.309 mmol, yield = 71%).^{1}H NMR (500 MHz, $CDCl_3$, 298 K): δ 9.91 (s, 1H), 8.23 (d, J = 6.0 Hz, 1H), 7.48 (dd, J = 7.6, 1.6 Hz, 1H), 7.13 – 7.05 (m, 2H), 7.03 (d, J = 2.5 Hz, 1H), 6.44 (dd, J = 6.1, 2.5 Hz, 1H), 3.44 (q, J = 7.1 Hz, 4H), 1.29 – 1.20 (m, 6H). ^{13}C NMR (125 MHz, $CDCl_3$, 298 K): δ 156.40, 156.23, 152.87, 149.24, 130.37, 128.61, 121.21, 120.81, 118.15, 109.73, 105.31, 102.03, 44.12, 12.55. FT-IR(ATR, cm^{-1}): 3172, 3074, 3022, 2972, 2926, 2870, 2853, 2767, 2690, 2531, 2346, 2324, 2243, 2187, 2179, 2163, 2115, 2087, 2051, 2039, 2011, 1980, 1919, 1892, 1871, 1846, 1827, 1794, 1694, 1620, 1592, 1537, 1505, 1480, 1448, 1398, 1377, 1357, 1303, 1267, 1252, 1197, 1177, 1159, 1138, 1097, 1078, 1059, 1027, 986, 911, 875, 834, 809. HRMS (ESI) calcd for $C_{16}H_{18}N_4O$ $[M+H]^+$ 283.1553, found 283.1555.

Scheme S5. Synthetic route to **BZ-5**.

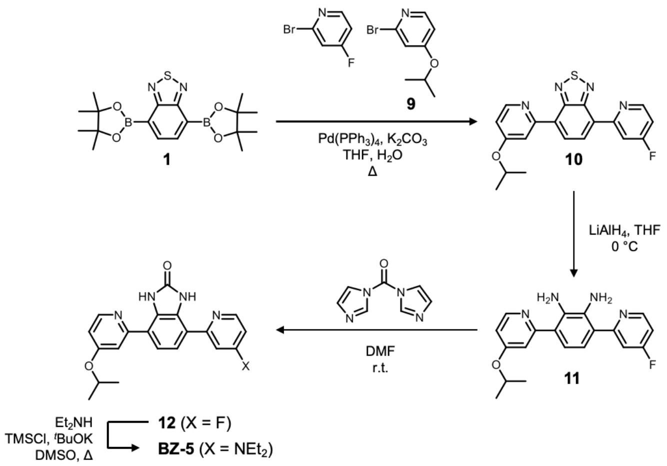

2-Bromo-4-isopropoxypyridine (9). A 250 mL round-bottom flask was charged with 2-bromo-4-hydroxypyridine (3.72 g, 21.4 mmol), 2-bromopropane (6 mL, 50 mmol), K_2CO_3 (5.99 g, 43.4 mmol), and MeCN (100 mL). The reaction mixture was stirred at 80 °C for 1 d, filtered with glass frit and Celite, washed with acetone, and concentrated under reduced pressure. Flash column chromatography on SiO_2 (hexane:EtOAc = 10:0 to 8:2, v/v) furnished **9** as a yellow liquid (4.20 g, 19.4 mmol, yield = 91%). ^1H NMR (500 MHz, $CDCl_3$, 298 K): δ 8.14 (d, J = 5.7 Hz, 1H), 6.96 (d, J = 2.3 Hz, 1H), 6.73 (dd, J = 5.8, 2.3 Hz, 1H), 4.60 (p, J = 6.1 Hz, 1H), 1.36 (d, J = 6.1 Hz, 6H). ^{13}C NMR (125 MHz, $CDCl_3$, 298 K): δ 165.33, 150.66, 142.99, 142.97, 114.37, 111.07, 70.86, 21.63. FT-IR(ATR, cm^{-1}): 3797, 3647, 3421, 3160, 3133, 3059, 2979, 2934, 2878, 2768, 2699, 2647, 2606, 2534, 2497, 2325, 2291, 2219, 2186, 2164, 2140, 2103, 2051, 2012, 1981, 1916, 1867, 1768, 1668, 1577, 1542, 1468, 1422, 1383, 1357, 1331, 1302, 1268, 1255, 1231, 1179, 1140, 1105, 1061, 984, 960, 914, 882, 868, 854, 835, 817, 800. HRMS (ESI) calcd for $C_8H_{10}BrNO$ $[M+H]^+$ 216.0019 and 217.9998, found 216.0021 and 218.0000.

4-(4-Fluoropyridin-2-yl)-7-(4-isopropoxypyridin-2yl)benzo[*c*][1,2,5]thiadiazole (10).[8] A 250 mL 3-neck round-bottom flask was charged with benzothiadiazole-4,7-bis(boronic acid pinacol ester) (**1**) (2.45 g, 6.30 mmol), **9** (2.72 g, 12.6 mmol), $Pd(PPh_3)_4$ (0.383 g, 0.331 mmol), K_2CO_3 (4.36 g, 31.6 mmol), water (6 mL), and dry THF (60 mL) under an argon atmosphere. 2-bromo-4-fluoropyridine (0.62 mL, 6.0 mmol) was added and the solution was stirred at 80 °C for 1 d. The reaction mixture was poured into water (100 mL), and extracted into CH_2Cl_2 (150 mL × 3). The combined organic layer was dried over anhyd Na_2SO_4, filtered, and concentrated under reduced pressure. Flash column chromatography on SiO_2 (hexane:EtOAc = 10:0 to 1:1, v/v) furnished **10** as a yellow solid (0.614 g, 1.68 mmol, yield = 27%). ^1H NMR (500 MHz, $CDCl_3$, 298 K): δ 8.76 (dd, J = 8.8, 5.5 Hz, 1H), 8.70 (d, J = 7.6 Hz, 1H), 8.68 – 8.57 (m, 3H), 8.29 (d, J = 2.4 Hz, 1H), 7.09 (ddd, J = 7.9, 5.6, 2.4 Hz, 1H), 6.85 (dd, J = 5.7, 2.4 Hz, 1H), 4.80 (hept, J = 6.0 Hz, 1H), 1.46

---

[8] To compensate for the reactivity difference between 2-bromo-4-fluoropyridine and 2-bromo-4-isopropoxypyridine, an optimized molar ratio of 0.95:2 was used for the synthesis of **10**.

(d, J = 6.1 Hz, 6H). ^{13}C NMR (125 MHz, $CDCl_3$, 298 K): δ 170.26, 168.18, 164.80, 156.95, 156.88, 155.35, 153.85, 153.65, 151.91, 151.86, 150.98, 133.09, 130.11, 129.63, 113.28, 113.13, 113.01, 110.98, 110.85, 110.50, 70.40, 21.97. FT-IR(ATR, cm^{-1}): 3727, 3185, 3104, 3064, 2978, 2924, 2852, 2633, 2359, 2342, 2325, 2287, 2187, 2163, 2141, 2051, 1981, 1912, 1716, 1593, 1570, 1544, 1493, 1460, 1424, 1406, 1386, 1374, 1346, 1313, 1298, 1276, 1261, 1224, 1179, 1140, 1112, 1053, 1006, 999, 991, 973, 945, 898, 872, 848, 819. HRMS (ESI) calcd for $C_{19}H_{15}FN_4OS$ [M+H]$^+$ 367.1026, found 367.1026.

3-(4-Fluoropyridin-2-yl)-6-(4-isopropoxypyridin-2-yl)benzene-1,2-diamine (11). An oven-dried 250 mL 3-neck round-bottom flask was charged with **10** (0.532 g, 1.45 mmol) and dry THF (80 mL) under an argon atmosphere. The solution was stirred at 0 °C, and dry $LiAlH_4$ (2 M in THF solution) (6 mL), was added dropwise over a period of 5 min. The reaction mixture was stirred at r.t. for 1 h and quenched with water (6 mL) at 0 °C. The mixture was poured CH_2Cl_2 (150 mL), dried over anhyd Na_2SO_4, filtered, and concentrated under reduced pressure. Flash column chromatography on SiO_2 (hexane:EtOAc = 2:1 to 1:1, v/v) furnished **11** as an orange solid (0.374 g, 1.00 mmol, yield = 76%). ^{1}H NMR (500 MHz, $CDCl_3$, 298 K): δ 8.62 (dd, J = 9.0, 5.6 Hz, 1H), 8.46 (d, J = 5.8 Hz, 1H), 7.46 (dd, J = 11.0, 2.4 Hz, 1H), 7.17 (d, J = 2.4 Hz, 1H), 7.12 – 7.05 (m, 2H), 6.95 (ddd, J = 8.2, 5.7, 2.4 Hz, 1H), 6.73 (dd, J = 5.8, 2.4 Hz, 1H), 5.64 (s, 4H), 4.72 (hept, J = 6.1 Hz, 1H), 1.41 (d, J = 6.1 Hz, 6H). ^{13}C NMR (125 MHz, $CDCl_3$, 298 K): δ 170.44, 168.36, 165.00, 162.80, 162.75, 160.95, 150.52, 150.46, 149.57, 137.08, 136.51, 124.22, 121.72, 121.69, 118.98, 118.82, 109.98, 109.93, 109.79, 109.31, 109.18, 109.14, 70.11, 21.96. FT-IR(ATR, cm^{-1}): 3710, 3402, 3277, 3069, 2978, 2932, 2647, 2511, 2374, 2360, 2342, 2325, 2187, 2163, 2139, 2051, 1999, 1981, 1963, 1919, 1847, 1590, 1574, 1560, 1492, 1462, 1443, 1395, 1375, 1326, 1301, 1258, 1229, 1179, 1159, 1140, 1107, 1059, 994, 948, 909, 867, 841, 821. HRMS (ESI) calcd for $C_{19}H_{19}FN_4O$ [M+H]$^+$ 339.1616, found 339.1617.

4-(4-Fluoropyridin-2-yl)-7-(4-isopropoxypyridin-2-yl)-1,3-dihydro-2*H*-benzo[*d*]imidazol-2-one (12). A 20 mL vial was charged with **11** (105 mg, 0.311 mmol), 1,1'-carbonyldiimidazole (198 mg, 1.22 mmol), and THF (10 mL). The reaction mixture was stirred at 40 °C for 2 d and concentrated under reduced pressure. Flash column chromatography on SiO_2 (hexane:EtOAc = 100:0 to 0:100, v/v) furnished **12** as a white solid (95.6 m g, 0.262 mmol, yield = 84%).^{1}H NMR (400 MHz, $CDCl_3$, 298 K): δ 10.54 (s, 2H), 10.34 (s, 2H), 8.64 (dd, J = 8.7, 5.7 Hz, 1H), 8.47 (dd, J = 5.7, 1.6 Hz, 1H), 7.63 (dd, J = 10.6, 2.3 Hz, 1H), 7.56 (dd, J = 7.2, 5.6 Hz, 2H), 7.40 (d, J = 2.3 Hz, 1H), 7.00 (ddd, J = 8.2, 6.0, 2.4 Hz, 1H), 6.76 (dd, J = 5.7, 2.3 Hz, 1H), 4.74 (h, J = 5.9 Hz, 1H), 1.43 (dt, J = 6.0, 1.0 Hz, 6H). ^{13}C NMR (125 MHz, $CDCl_3$, 298 K): δ 170.51, 168.42, 164.97, 159.03, 158.98, 157.08, 154.90, 151.55, 151.49, 150.45, 129.84, 129.76, 120.13, 118.24, 118.12, 110.16, 110.03, 109.30, 107.74, 107.49, 107.34, 70.35, 21.94. FT-IR(ATR, cm^{-1}): 3388, 3197, 3145, 3071, 3021, 2979, 2937, 2635, 2325, 2284, 2239, 2163, 2103, 2051, 2040, 2013, 1980, 1951, 1914, 1854, 1743, 1720, 1629, 1598, 1573, 1520, 1485, 1467, 1412, 1387, 1360, 1313, 1274, 1261, 1222, 1172, 1139, 1109, 1077, 1013, 997, 981, 957, 932, 913, 881, 857, 825. HRMS (ESI) calcd for $C_{20}H_{17}FN_4O_2$ [M+H]$^+$ 365.1408, found 365.1412.

4-(4-(Diethylamino)pyridin-2-yl)-7-(4-isopropoxypyridin-2-yl)-1,3-dihydro-2*H*-benzo[*d*]imidazol-2-one (BZ-5). A 10–20 mL Biotage® Microwave Reaction Vial was charged with **12** (71.0 mg, 0.195 mmol), dietylamine (0.8 mL, 4 mmol), TMSCl (0.4 mL, 3 mmol), KO$_t$Bu (50.3 mg, 0.448 mmol), and DMSO (7 mL) under argon sparge. The mixture was heated by microwave irradiation at 100 °C with stirring for 12 h, cooled to r.t., poured into EtOAc (100 mL), and washed with water (75 mL × 3). The organic layer was dried over anhyd Na_2SO_4, filtered, and concentrated under reduced pressure. Flash column chromatography on SiO_2 (hexane:acetone = 10:0 to 1:1, v/v) furnished **BZ-5** as a white-yellow solid (33.6 mg, 0.0805 mmol, yield = 41%).^{1}H

NMR (500 MHz, $CDCl_3$, 298 K): δ 10.44 (s, 1H), 8.46 (d, J = 5.9 Hz, 1H), 8.25 (d, J = 6.1 Hz, 1H), 7.53 (s, 2H), 7.38 (d, J = 2.3 Hz, 1H), 7.06 (s, 1H), 6.76 – 6.71 (m, 1H), 6.46 (d, J = 6.2 Hz, 1H), 4.77 – 4.71 (m, 1H), 3.46 (q, J = 7.2 Hz, 4H), 1.42 (d, J = 6.1 Hz, 6H), 1.25 (t, J = 7.1 Hz, 6H). ^{13}C NMR (125 MHz, $CDCl_3$, 298 K): δ 164.89, 157.59, 156.01, 155.05, 152.85, 150.43, 149.29, 129.85, 129.72, 120.76, 119.05, 117.89, 117.85, 109.00, 107.46, 105.40, 102.18, 70.26, 44.14, 29.84, 21.95, 12.57. FT-IR(ATR, cm^{-1}): 3746, 3356, 3088, 3073, 2973, 2924, 2870, 2854, 2524, 2325, 2287, 2239, 2163, 2139, 2115, 2083, 2066, 2051, 2011, 1992, 1980, 1967, 1943, 1910, 1896, 1868, 1811, 1780, 1767, 1704, 1642, 1588, 1557, 1537, 1522, 1500, 1468, 1434, 1416, 1377, 1357, 1303, 1252, 1226, 1194, 1159, 1140, 1109, 1084, 1027, 1010, 994, 988, 937, 910, 874, 863, 801. HRMS (ESI) calcd for $C_{24}H_{27}N_5O_2$ $[M+H]^+$ 418.2238, found 418.2239.

X-ray Crystallographic Studies on BZ-3. Single crystals of **BZ-3** were prepared by slow diffusion of methyl *tert*-butyl ether into a $CHCl_3$ solution of this material. A colorless crystal (approximate dimensions 0.587 × 0.416 × 0.357 mm^3) was placed onto a nylon loop with Paratone-N oil, and mounted on an XtaLAB AFC12 (RINC): Kappa dual home/near diffractometer. The data collection was carried out using Cu Kα radiation and the crystal was kept at $T = 93$ K. A total of 19770 reflections were measured ($7.896° \leq 2\theta \leq 158.828°$). The structure was solved with SHELXT[9] using direct methods, and refined with SHELXL[10] refinement package of OLEX2.[11] A total of 5672 unique reflections were used in all calculations. The final $R1$ was 0.0657 ($I \geq 2\sigma(I)$) and $wR2$ was 0.1841 (all data). CCDC 2367198 contains the supplementary crystallographic data for this structure.

---

[9] G. M. Sheldrick, *Acta Cryst.*, 2015, **A71**, 3–8.

[10] G. M. Sheldrick, *Acta Cryst.*, 2015, **C71**, 3–8.

[11] O. V. Dolomanov, L. J. Bourhis, R. J. Gildea, J. A. K. Howard, and H. Puschmann, *J. Appl. Cryst.*, 2009, **42**, 339–341.

Table S1. Photophysical properties of compounds **BZ-1**, **BZ-2**, **BZ-3**, **BZ-4** and **BZ-5** in CH_2Cl_2 at T = 298 K.

	$\lambda_{\mathrm{max,abs}}$ (nm)[a]	ε (M^{-1} cm^{-1})	$\Delta\nu$ (cm^{-1})	$\lambda_{\mathrm{max,em}}$ (nm)	$\varPhi_{\mathrm{F}}$[b]
BZ-1	380	9000	3894	446	0.01
BZ-2	324	56800	–	–	–
BZ-3	312	25800	12405	509	0.21
BZ-4	314	6220	12123	507	0.24
BZ-5	314	22800	12579	519	0.22

[a] The longest absorption wavelength.

[b] Absolute fluorescence quantum yields determined by a calibrated integrating sphere system.

Table S2. Solvent-dependent photophysical properties of **BZ-3** (T = 298 K).

solvent	$\lambda_{\mathrm{max,abs}}$ (nm)	$\lambda_{\mathrm{max,em}}$ (nm)	$\nu_{\mathrm{max,em}}$ (cm^{-1})
cyclohexane	313	531	18832
EtOAc	312	491	20366
CH_2Cl_2	310	509	19646
MeOH	312	497	20120

Table S3. Summary of X-ray crystallographic data of **BZ-3**.

	BZ-3 · $CHCl_3$
Chemical formula	$C_{25}H_{30}N_6O \cdot CHCl_3$
Formula weight	549.92
Crystal system	monoclinic
Space group	$P2_1/n$
Color of crystal	colorless
a (Å)	12.18070(10)
b (Å)	11.62690(10)
c (Å)	19.3144(2)
β (°)	102.2310(10)
Volume (Å^3)	2673.29(4)
Z	4
R_{int}	0.0741
Final R indices [$I > 2\sigma(I)$]	$R1 = 0.0657$, $wR2 = 0.1816$
Final R indices [all data]	$R1 = 0.0676$, $wR2 = 0.1841$
Goodness-of-fit on F^2	1.065

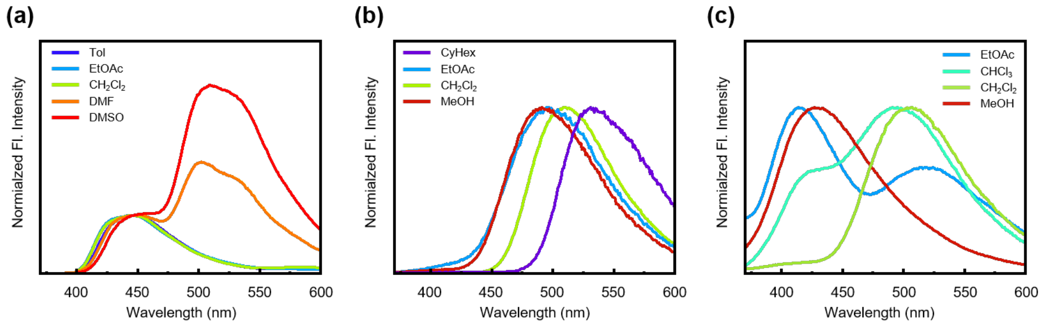

Fig. S1. Normalized emission spectra of (a) **BZ-1**, (b) **BZ-3**, and (c) **BZ-4** in different solvents at T = 298 K.

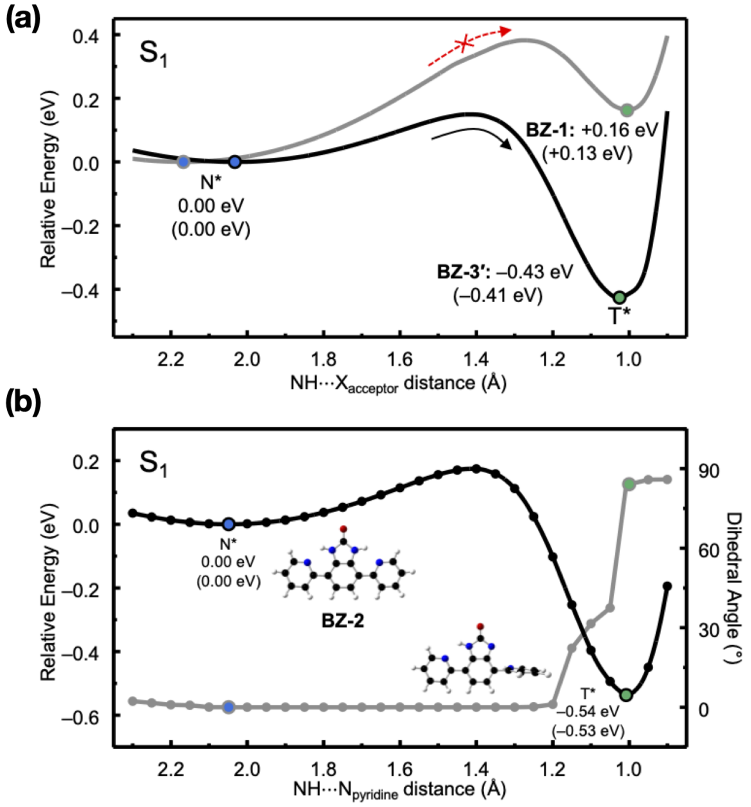

Fig. S2. (a) Potential energy curves of the S_1 state constructed at the TD-B3LYP-D3/6-31++G(d,p) level of theory with implicit solvation (CPCM) in CH_2Cl_2 by a relaxed scan along the fixed NH$\cdots$$X_{acceptor}$ distance (step = 0.05 Å). X = O (**BZ-1**); N (**BZ-3′**). (b) Potential energy curve (black line) and dihedral angle between the benzimidazolone and pyridine (gray line) of **BZ-2** in the S_1 state constructed at the TD-B3LYP-D3/6-31++G(d,p) level of theory with implicit solvation (CPCM) in CH_2Cl_2 by a relaxed scan along the fixed NH···$N_{pyridine}$ distance (step = 0.05 Å). Relative electronic energies of the stationary points (lined circles) are given, and the numbers in parenthesis indicate relative Gibbs free energy values.

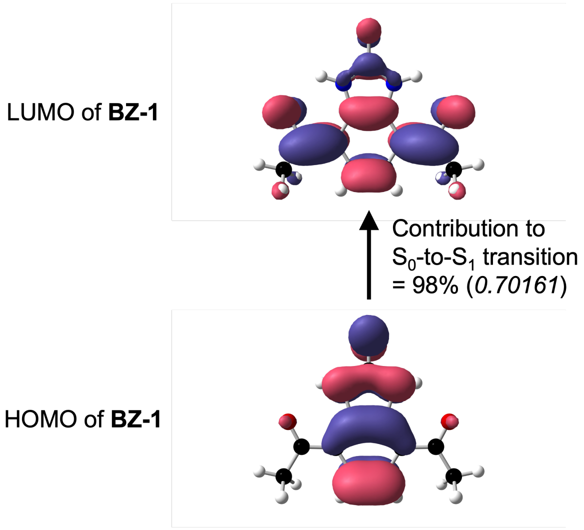

Fig. S3. Frontier molecular orbitals (FMOs) involved in the transition to the S_1 excited state of **BZ-1** calculated at the TD-B3LYP-D3/6-31G++G(d,p) level of theory with implicit solvation (CPCM) in CH_2Cl_2. The contribution of the HOMO→LUMO electronic transition to the S_0-to-S_1 transition is shown, with the number in parentheses denoting the CI (configurational interaction) expansion coefficient.

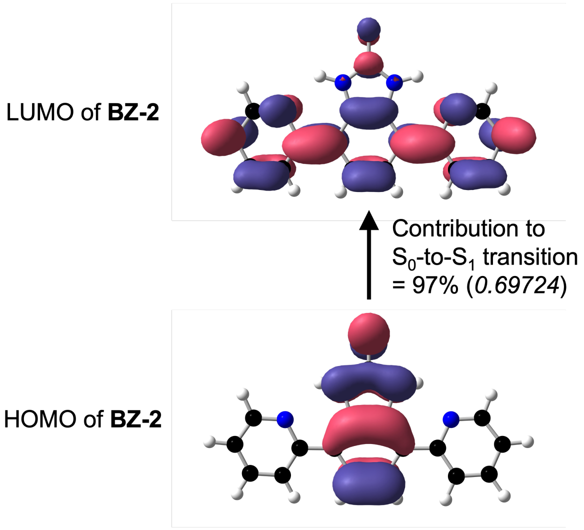

Fig. S4. Frontier molecular orbitals (FMOs) involved in the transition to the S_1 excited state of **BZ-2** calculated at the TD-B3LYP-D3/6-31G++G(d,p) level of theory with implicit solvation (CPCM) in CH_2Cl_2. The contribution of the HOMO→LUMO electronic transition to the S_0-to-S_1 transition is shown, with the number in parentheses denoting the CI (configurational interaction) expansion coefficient.

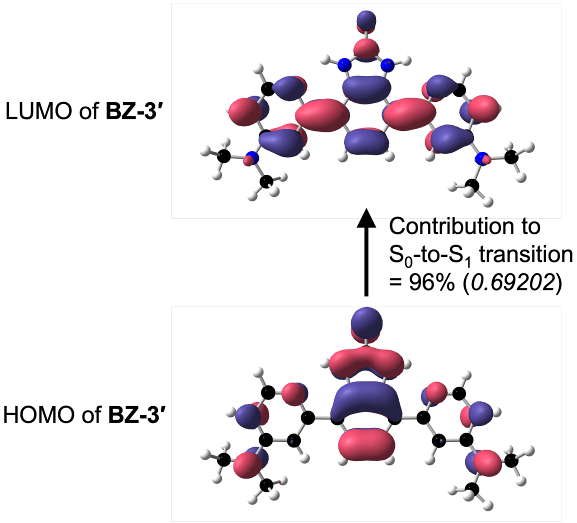

Fig. S5. Frontier molecular orbitals (FMOs) involved in the transition to the S_1 excited state of **BZ-3′** calculated at the TD-B3LYP-D3/6-31G++G(d,p) level of theory with implicit solvation (CPCM) in CH_2Cl_2. The contribution of the HOMO→LUMO electronic transition to the S_0-to-S_1 transition is shown, with the number in parentheses denoting the CI (configurational interaction) expansion coefficient.

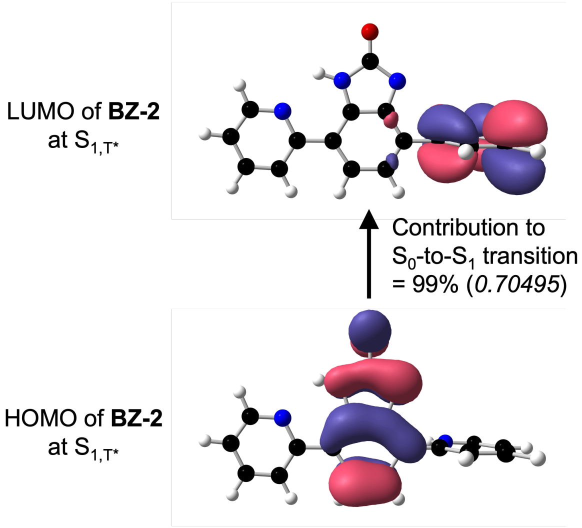

Fig. S6. Frontier molecular orbitals (FMOs) involved in the transition to the S_1 excited state of **BZ-2** at T* geometry calculated at the TD-B3LYP-D3/6-31G++G(d,p) level of theory with implicit solvation (CPCM) in CH_2Cl_2. The contribution of the HOMO→LUMO electronic transition to the S_0-to-S_1 transition is shown, with the number in parentheses denoting the CI (configurational interaction) expansion coefficient.

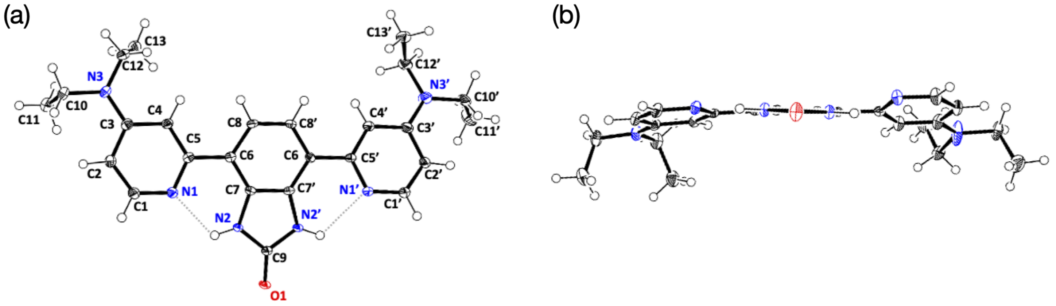

Fig. S7. X-ray structure of **BZ-3** as ORTEP diagrams with thermal ellipsoids at the 50% probability level: (a) face-on view; (b) edge-on view. Interatomic distances: N1···N2, 2.709(3) Å; N1′···N2′, 2.809(2) Å. Dihedral angles: 10.54° (N1–C5–C6–C7); 20.93° (N1′–C5′–C6′–C7′). One of the ethyl groups is disordered over two positions, for which only one is shown for clarity.

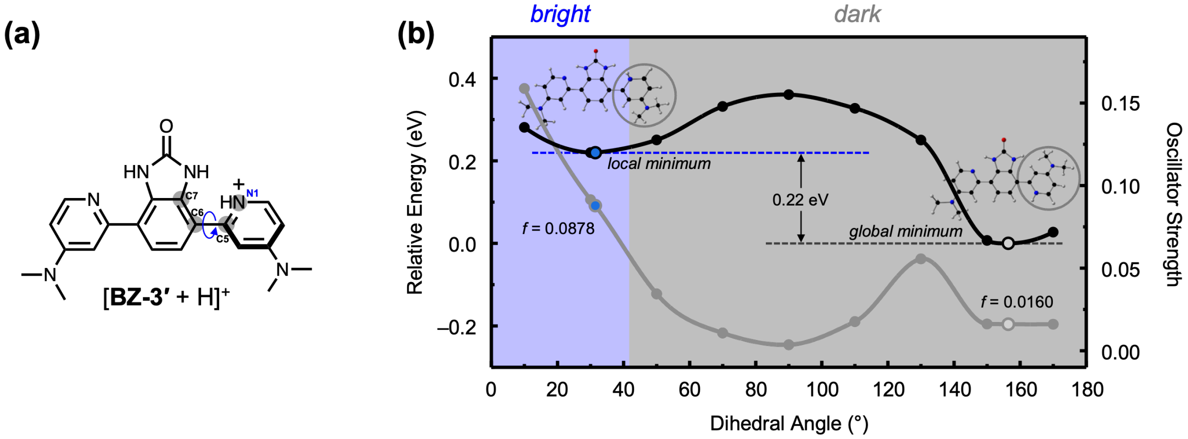

Fig. S8. (a) Chemical structure of the protonated DFT model **BZ-3′**. In scanning the dihedral angle, the C–C bond denoted with a blue arrow was rotated. (b) Potential energy curve (black line) and oscillator strength (f; gray line) of **BZ-3′** at the S_1 state, constructed at the TD-B3LYP-D3/6-31++G(d,p) level of theory with implicit solvation (CPCM) in CH_2Cl_2, by a relaxed scan along the fixed C7–C6–C5–N1 dihedral angle (step = 20°). Blue and gray lined circles indicate stationary points with optimized geometries shown next. Blue and gray shades indicate bright ($f > 0.06$) and dark ($f < 0.06$) regions, respectively.

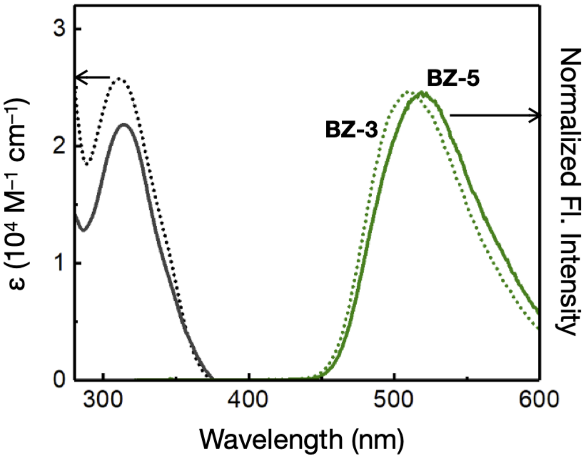

Fig. S9. Absorption and normalized emission spectra of **BZ-5** (solid lines) and **BZ-3** (dotted lines) in CH_2Cl_2. T = 298 K.

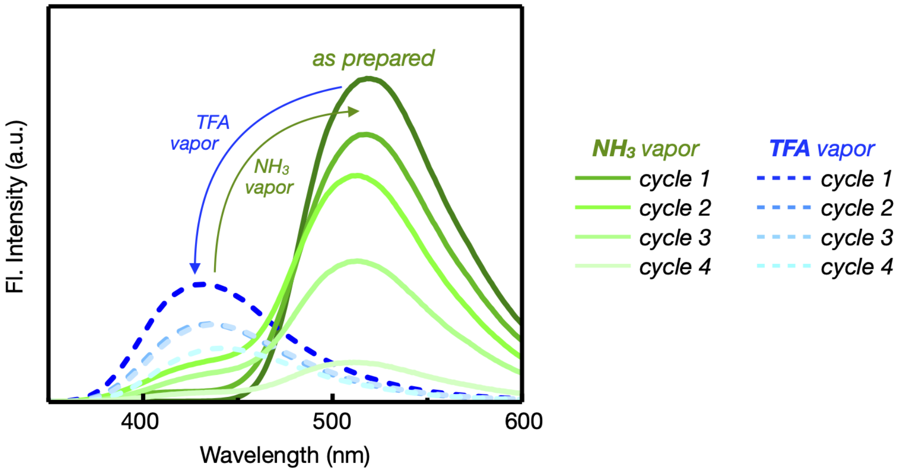

Fig. S10. Emission spectra (λ_{exc} = 310 nm) of the **BZ-5**-doped (10 wt%) PMMA film obtained during alternative cycles of exposure to saturated TFA (1 min) and NH_3 (5 min) repeated under ambient conditions.

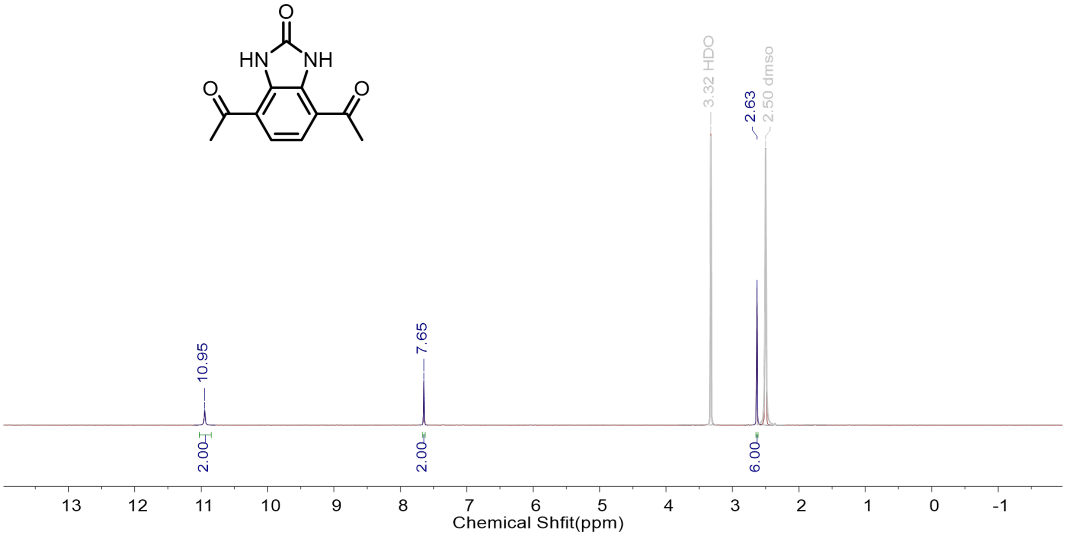

Figure S11. ^{1}H NMR (500 MHz) spectrum of **BZ-1** in DMSO-d_6 (T = 298 K).

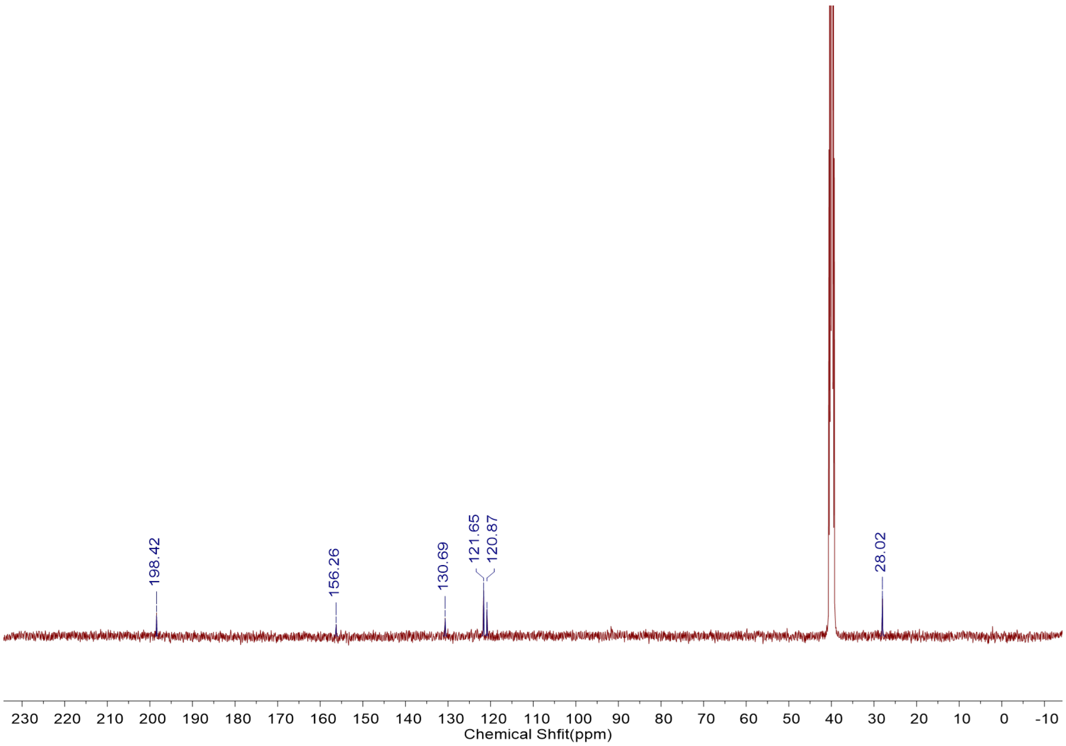

Figure S12. ^{13}C NMR (100 MHz) spectrum of **BZ-1** in DMSO-d_6 (T = 298 K).

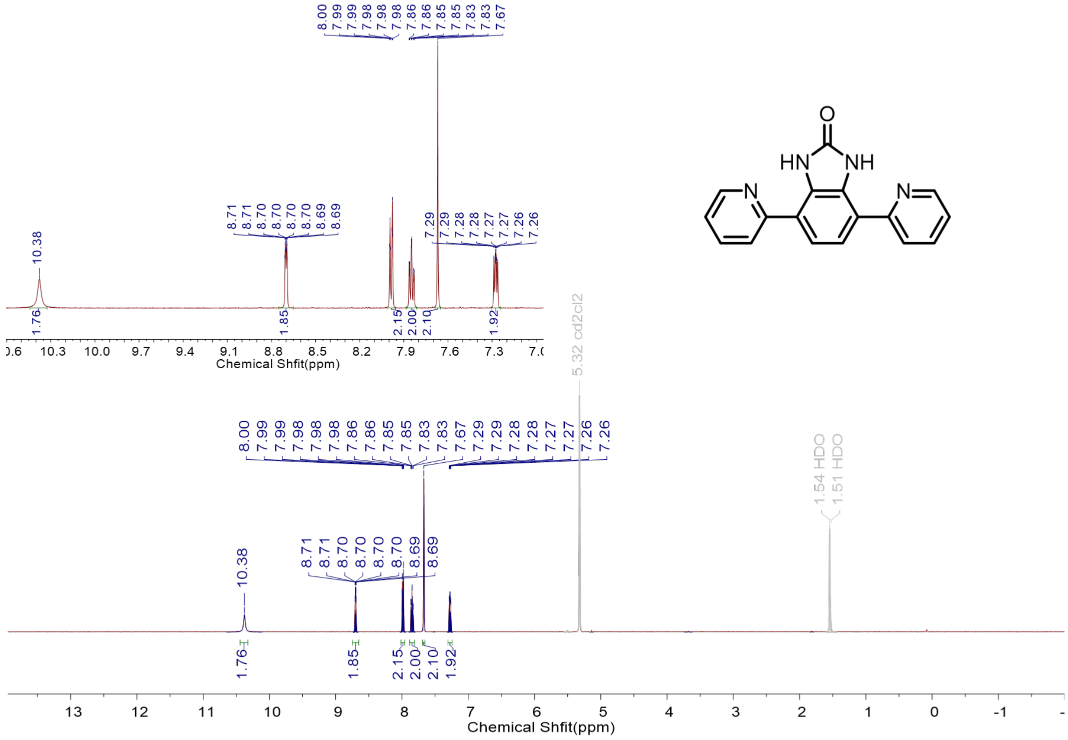

Figure S13. ^{1}H NMR (500 MHz) spectrum of **BZ-2** in CD_2Cl_2 (T = 298 K).

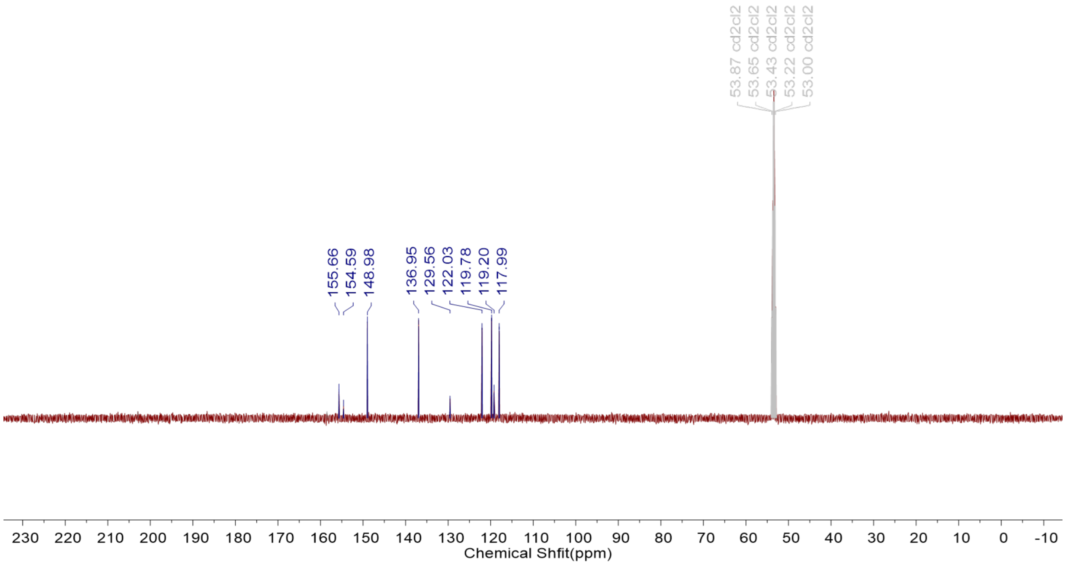

Figure S14. ^{13}C NMR (125 MHz) spectrum of **BZ-2** in CD_2Cl_2 (T = 298 K).

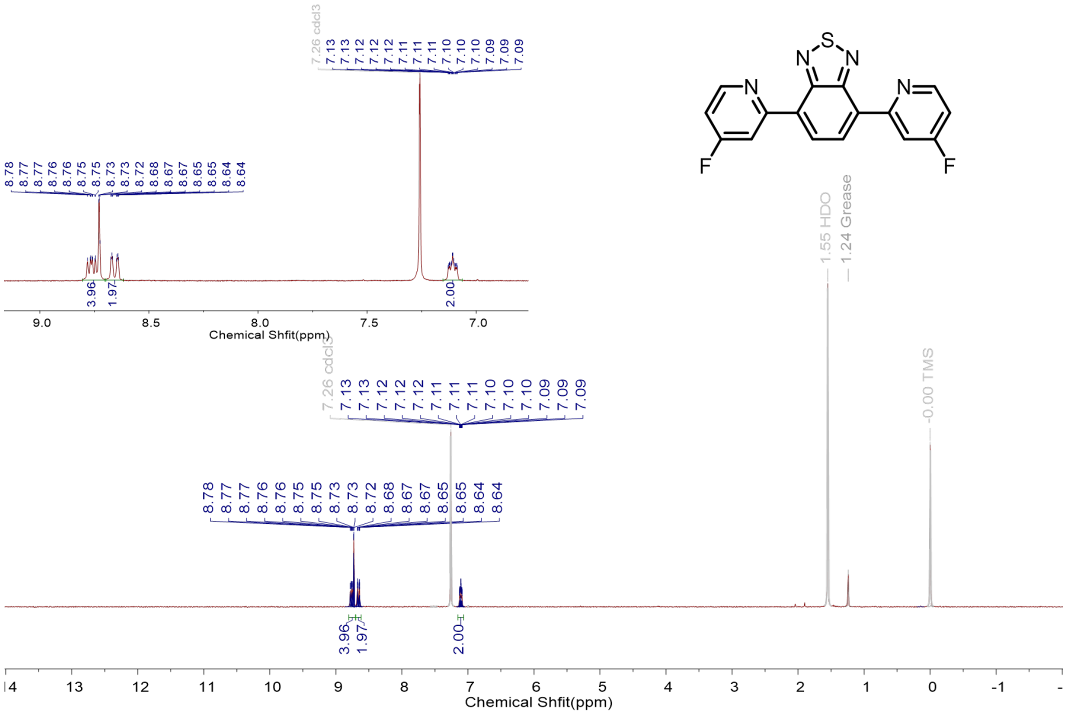

Figure S15. ^{1}H NMR (400 MHz) spectrum of **2** in $CDCl_3$ (T = 298 K).

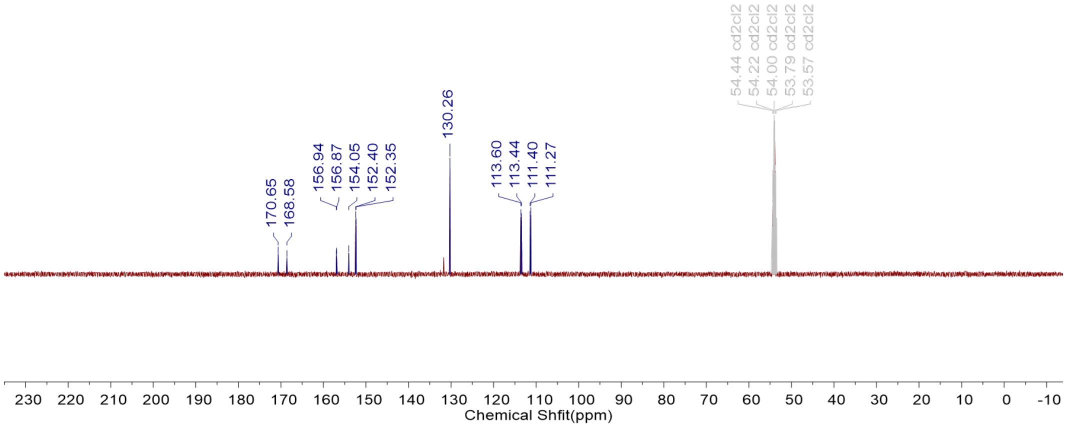

Figure S16. ^{13}C NMR (125 MHz) spectrum of **2** in CD_2Cl_2 (T = 298 K).

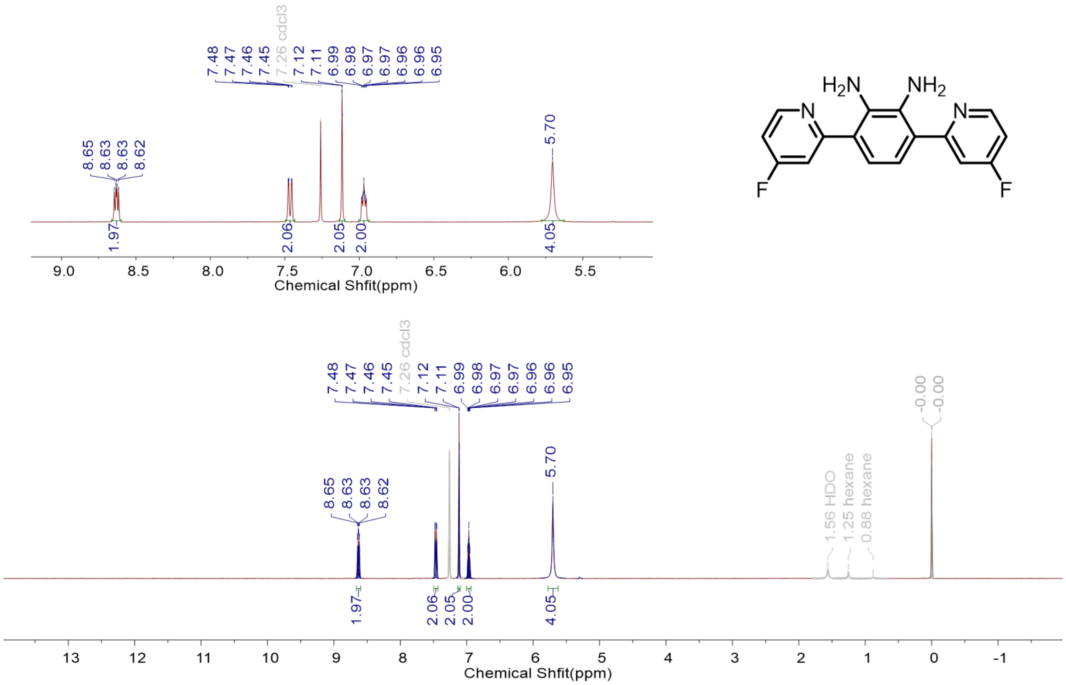

Figure S17. ^{1}H NMR (500 MHz) spectrum of **3** in $CDCl_3$ (T = 298 K).

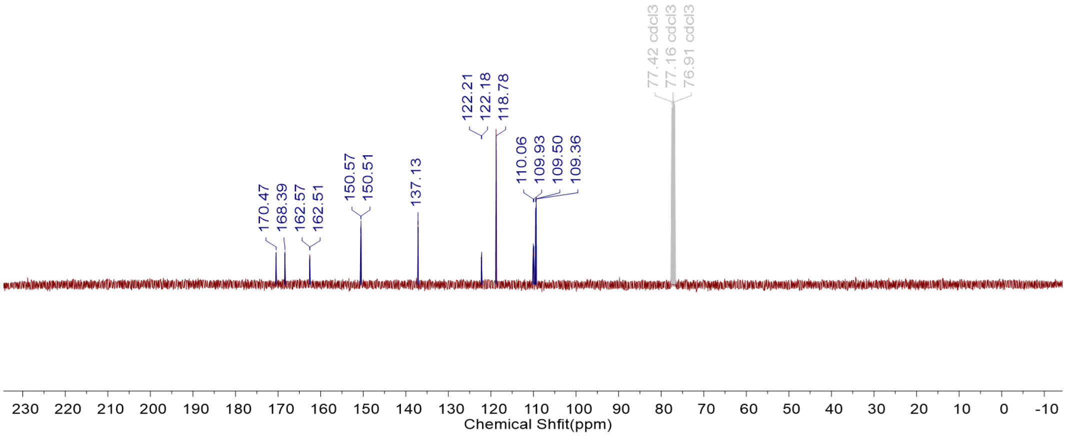

Figure S18. ^{13}C NMR (125 MHz) spectrum of **3** in $CDCl_3$ (T = 298 K).

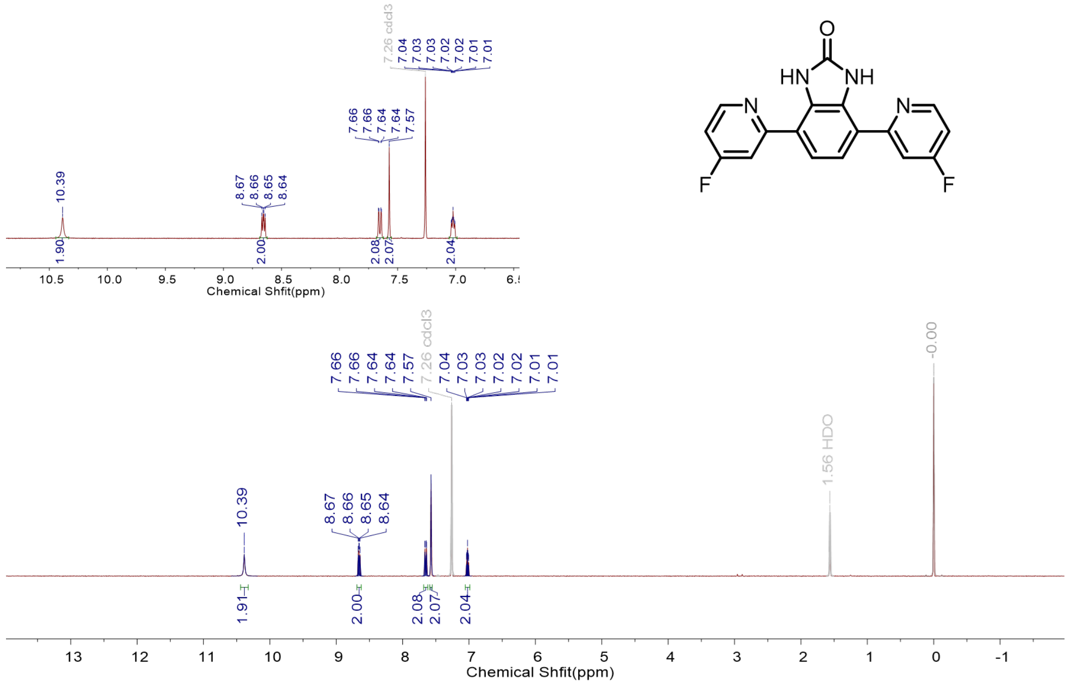

Figure S19. ^{1}H NMR (500 MHz) spectrum of **4** in $CDCl_3$ (T = 298 K).

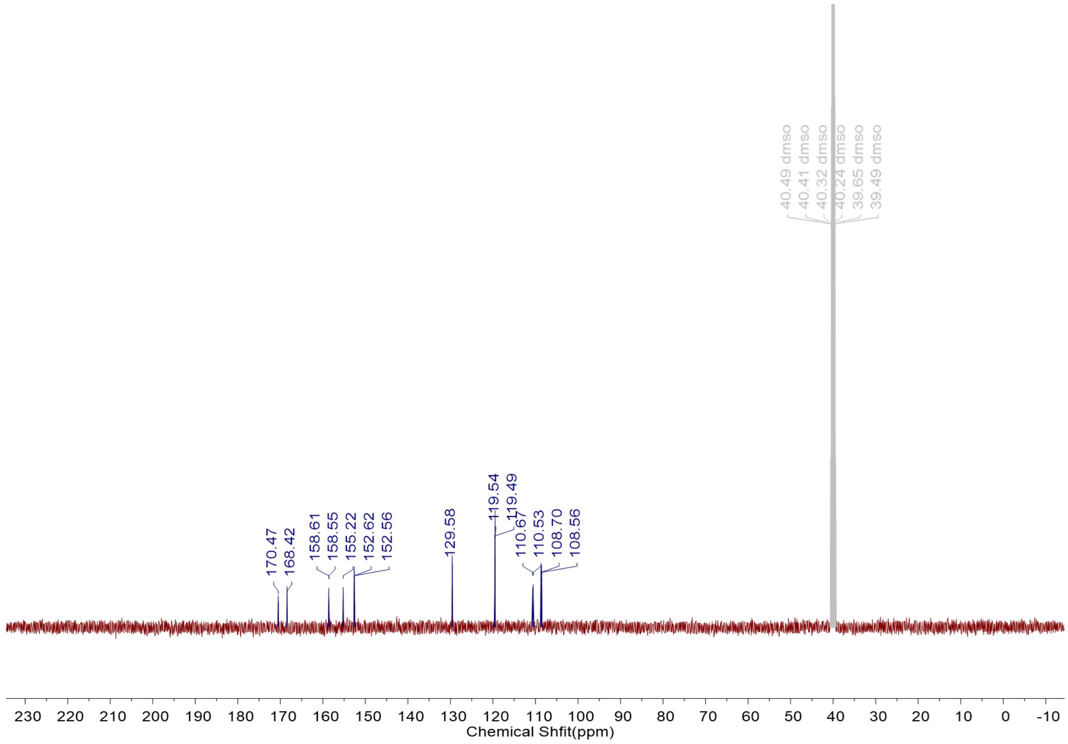

Figure S20. ^{13}C NMR (125 MHz) spectrum of **4** in DMSO-d_6 (T = 298 K).

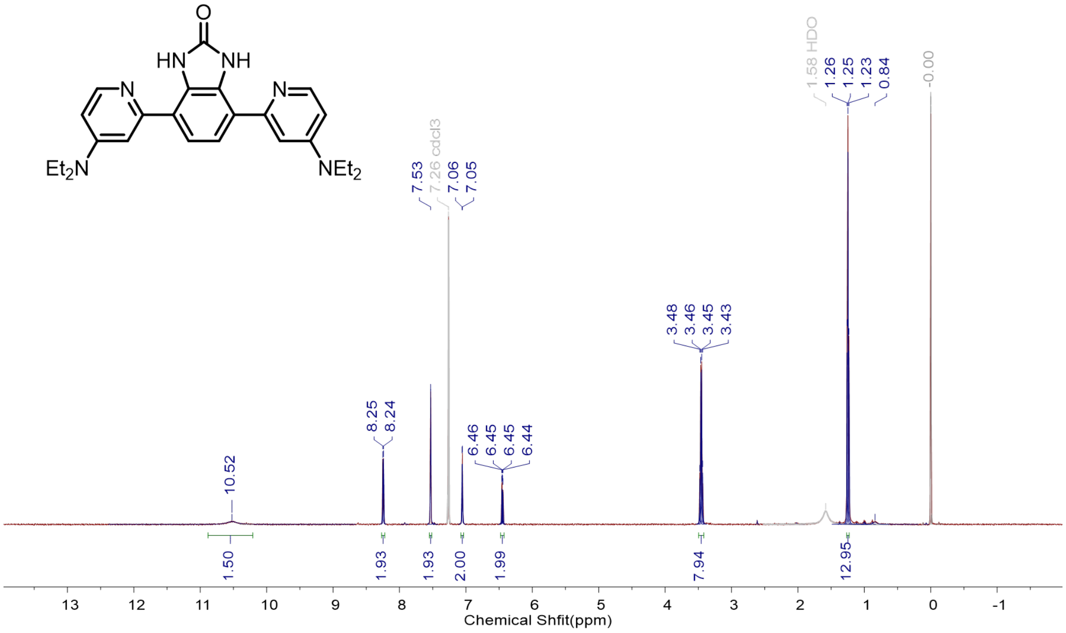

Figure S21. ^{1}H NMR (500 MHz) spectrum of **BZ-3** in $CDCl_3$ (T = 298 K).

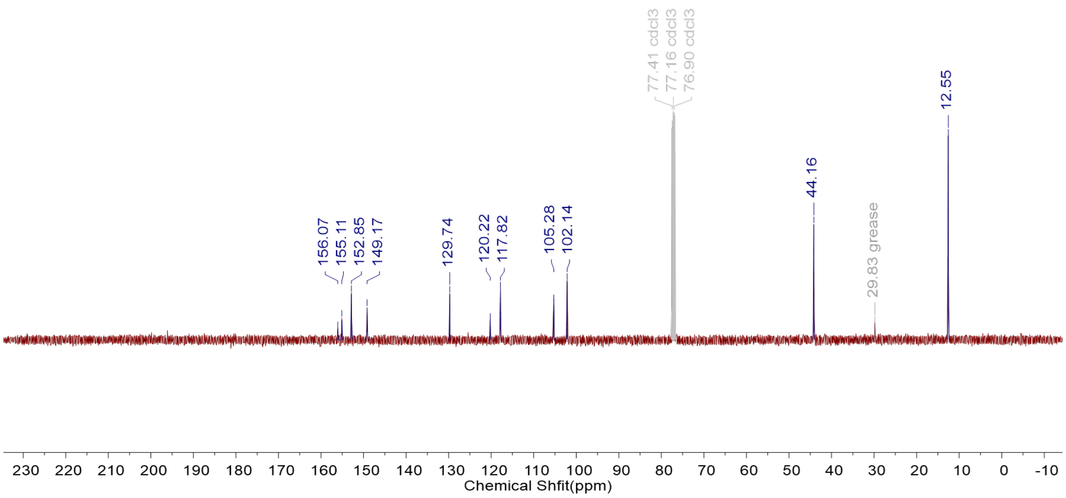

Figure S22. ^{13}C NMR (125 MHz) spectrum of **BZ-3** in $CDCl_3$ (T = 298 K).

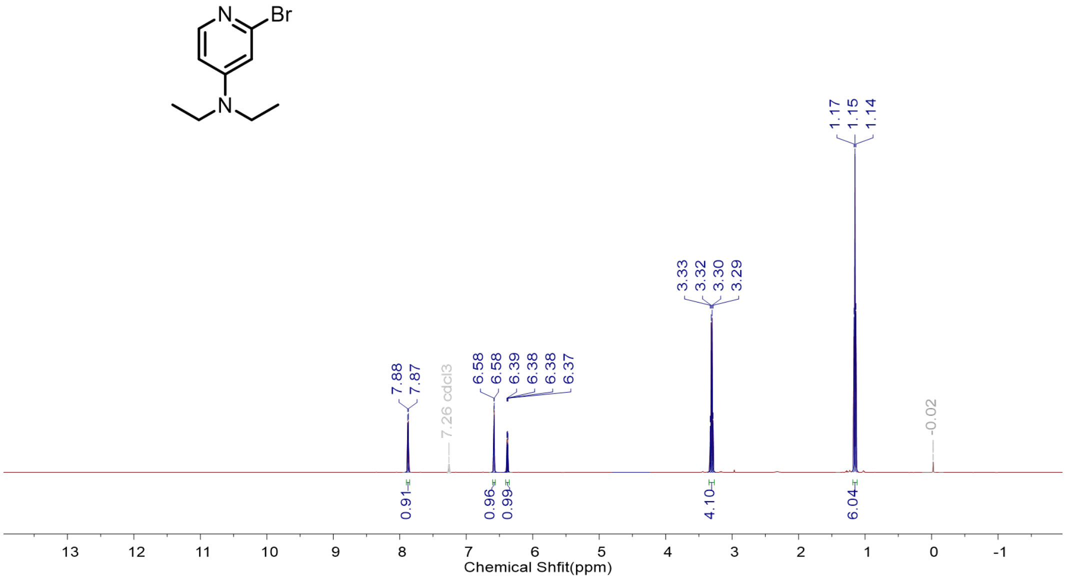

Figure S23. ^{1}H NMR (500 MHz) spectrum of **6** in $CDCl_3$ (T = 298 K).

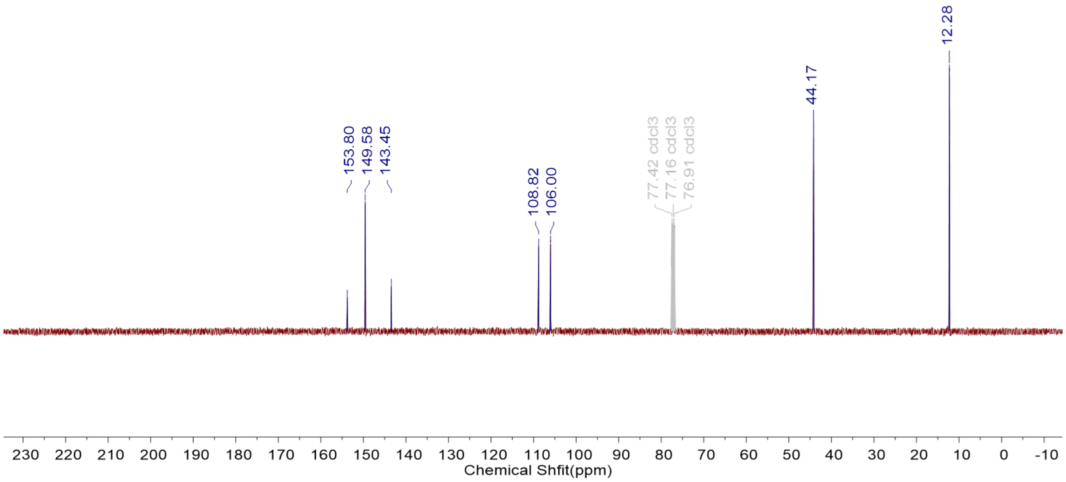

Figure S24. ^{13}C NMR (125 MHz) spectrum of **6** in $CDCl_3$ (T = 298 K).

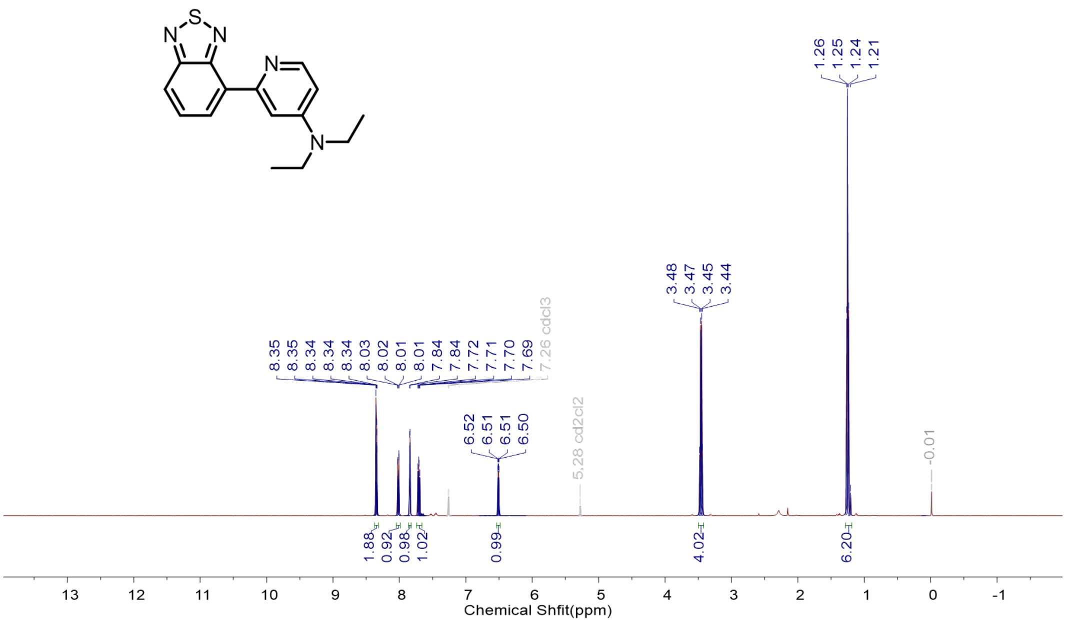

Figure S25. ^{1}H NMR (500 MHz) spectrum of **7** in $CDCl_3$ (T = 298 K).

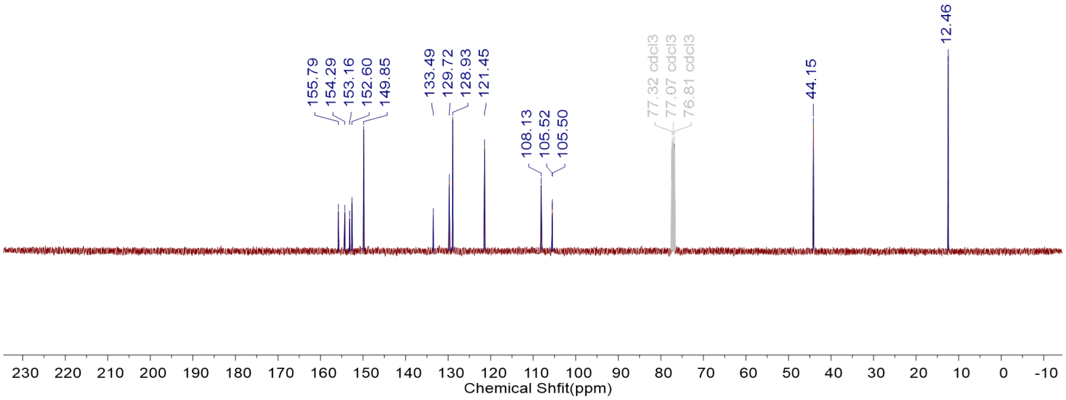

Figure S26. ^{13}C NMR (125 MHz) spectrum of **7** in $CDCl_3$ (T = 298 K).

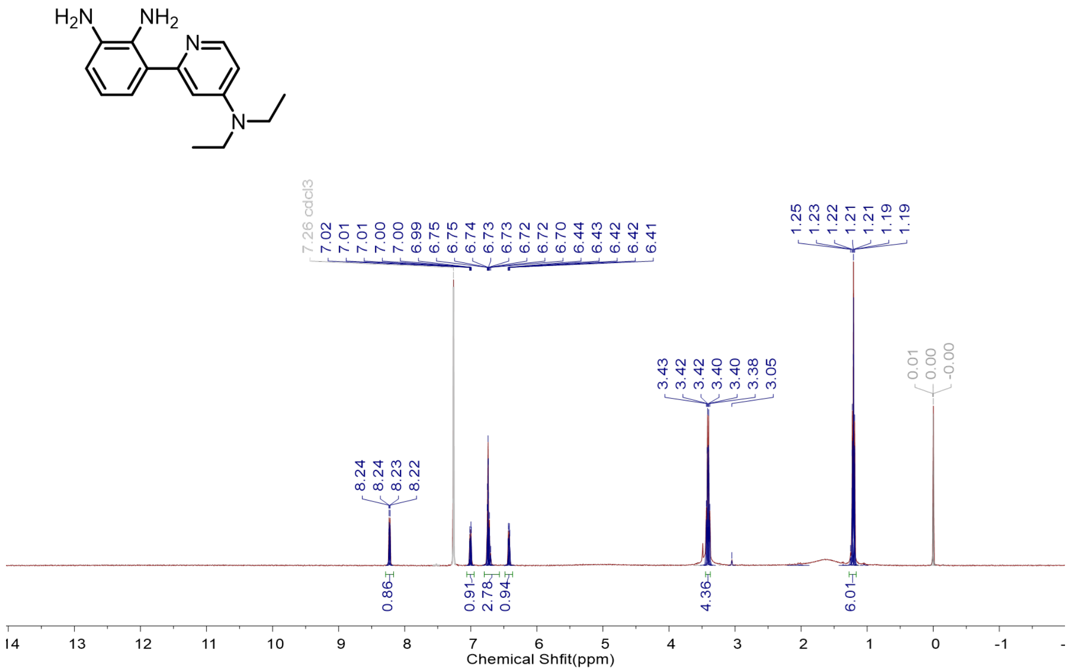

Figure S27. ^{1}H NMR (400 MHz) spectrum of **8** in $CDCl_3$ (T = 298 K).

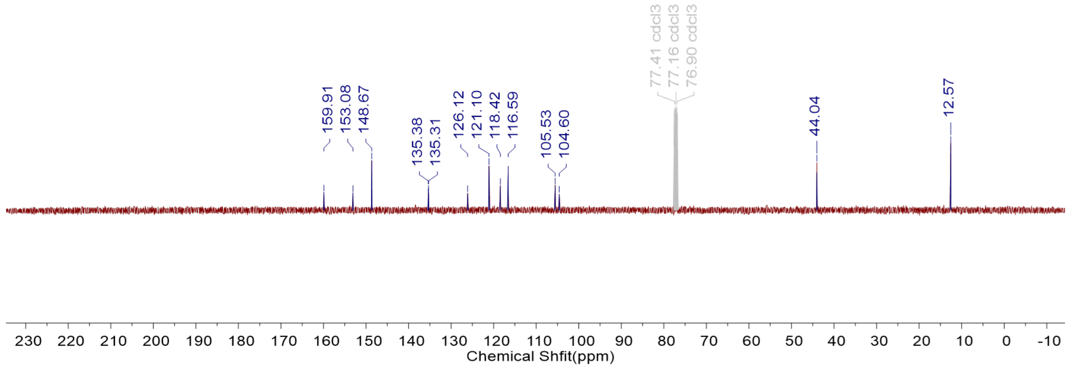

Figure S28. ^{13}C NMR (125 MHz) spectrum of **8** in $CDCl_3$ (T = 298 K).

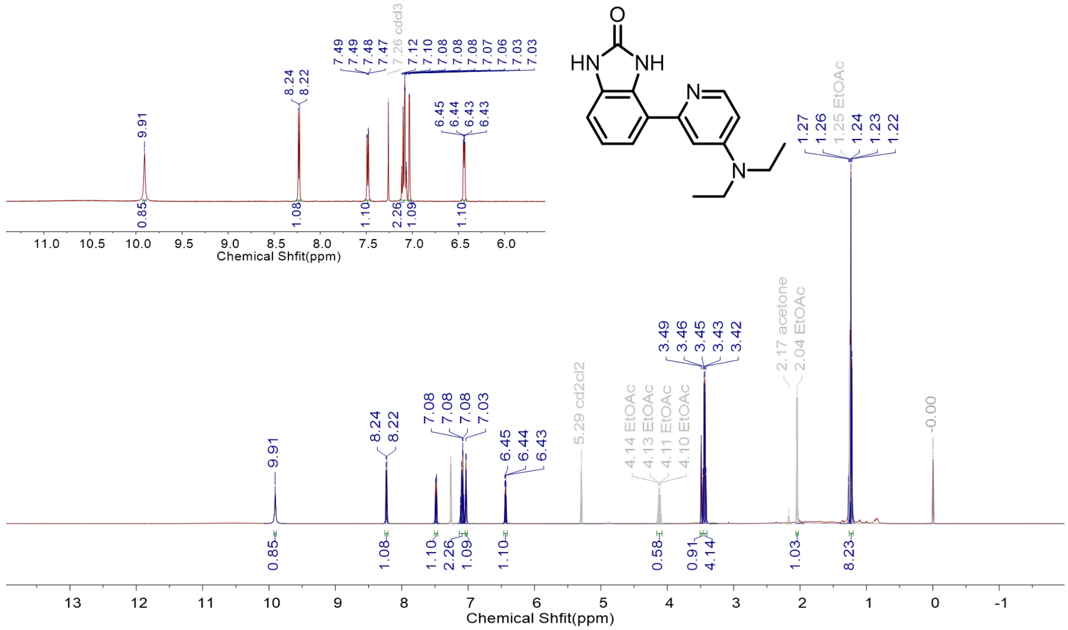

Figure S29. ^{1}H NMR (500 MHz) spectrum of **BZ-4** in CDCl$_3$ (T = 298 K).

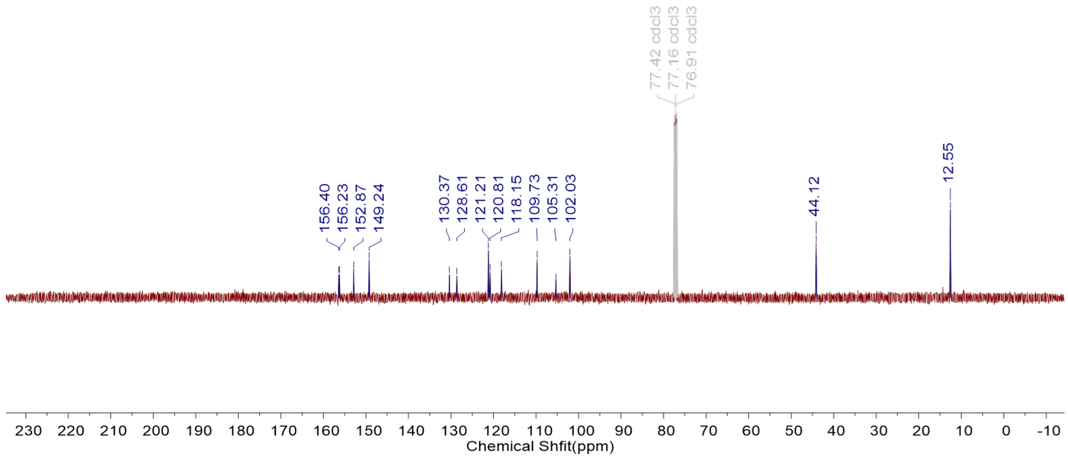

Figure S30. ^{13}C NMR (125 MHz) spectrum of **BZ-4** in CDCl$_3$ (T = 298 K).

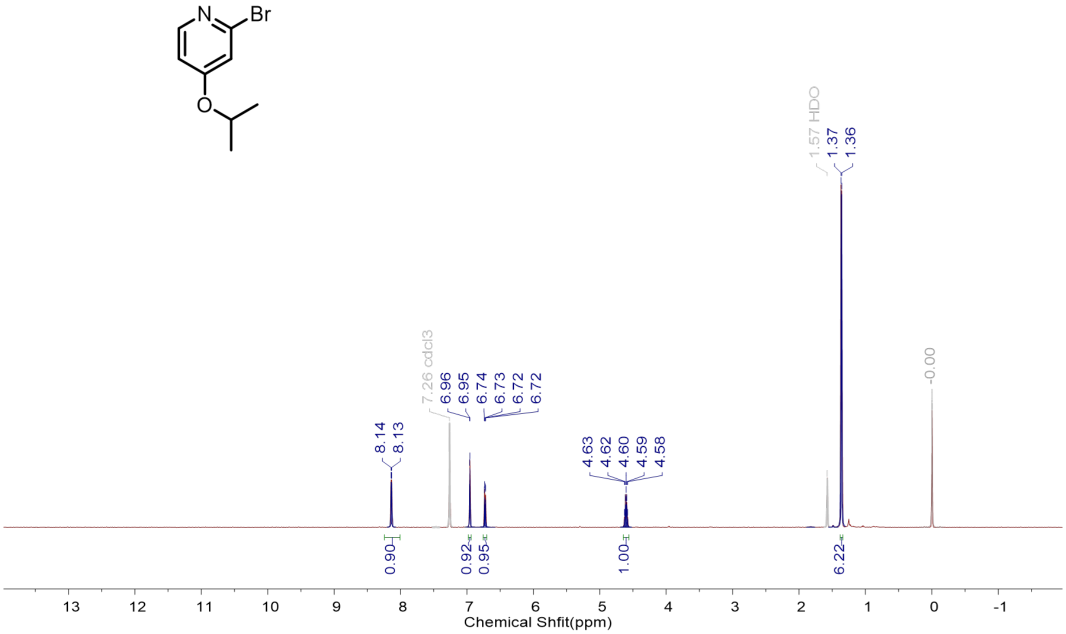

Figure S31. ^{1}H NMR (500 MHz) spectrum of **9** in $CDCl_3$ (T = 298 K).

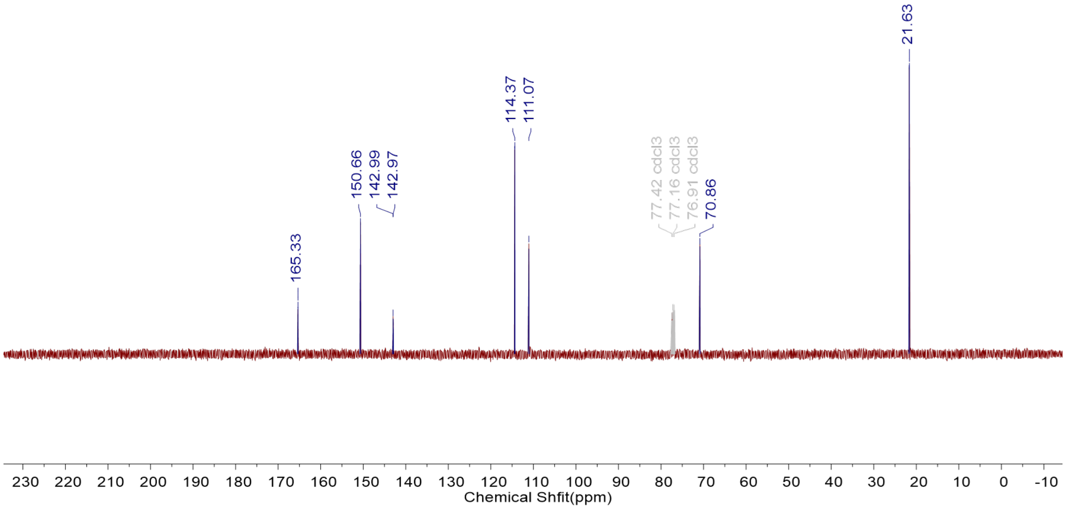

Figure S32. ^{13}C NMR (125 MHz) spectrum of **9** in $CDCl_3$ (T = 298 K).

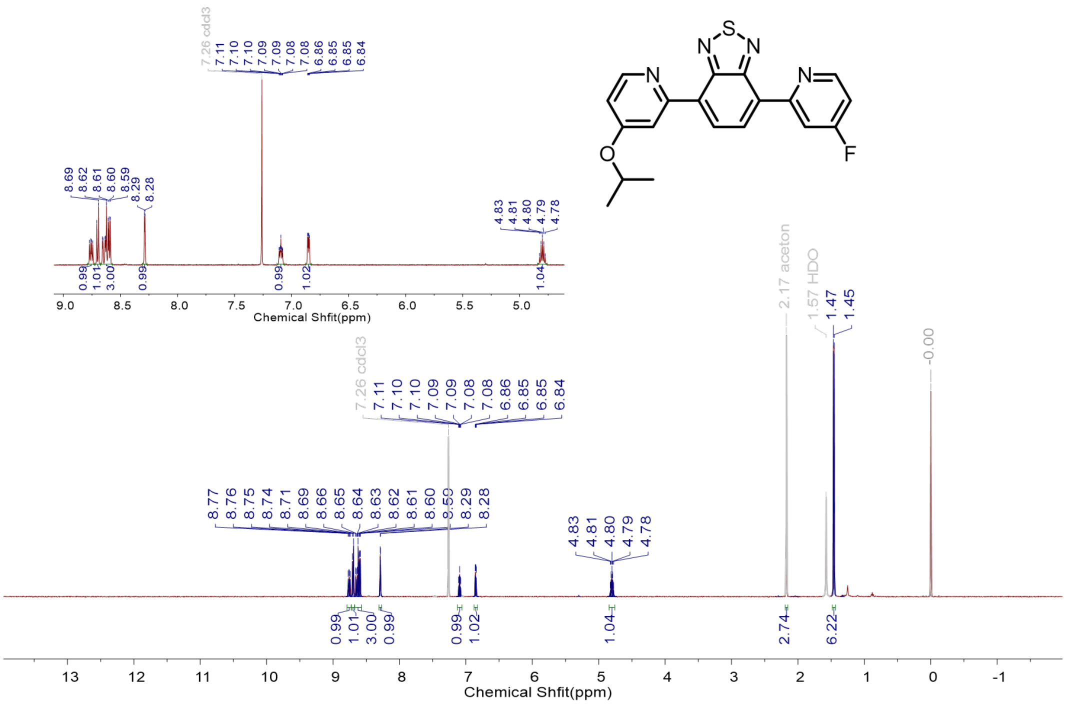

Figure S33. ^{1}H NMR (500 MHz) spectrum of **10** in CDCl$_3$ (T = 298 K).

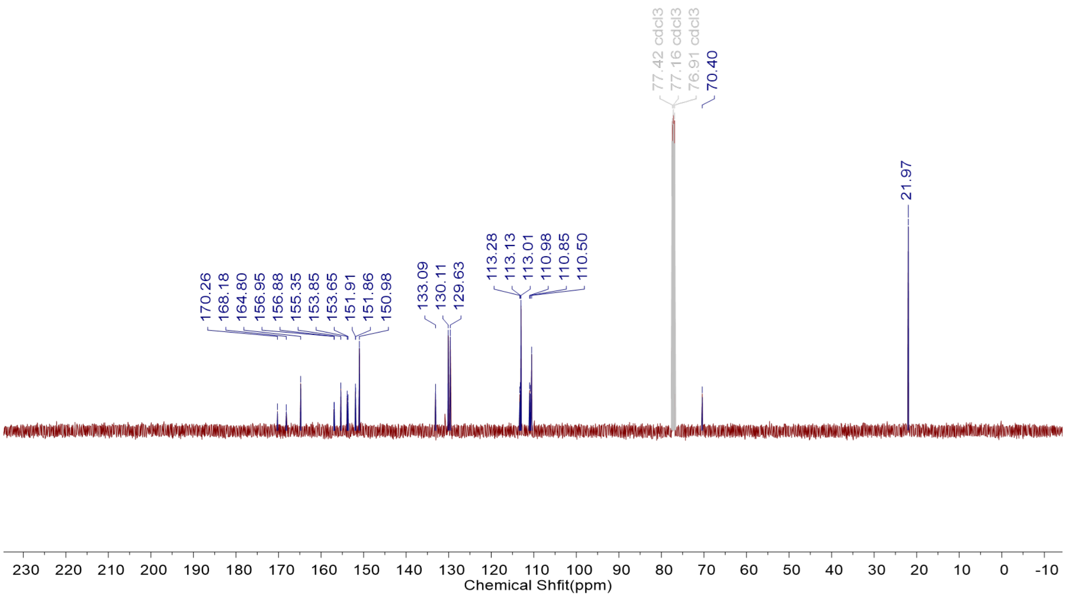

Figure S34. ^{13}C NMR (125 MHz) spectrum of **10** in CDCl$_3$ (T = 298 K).

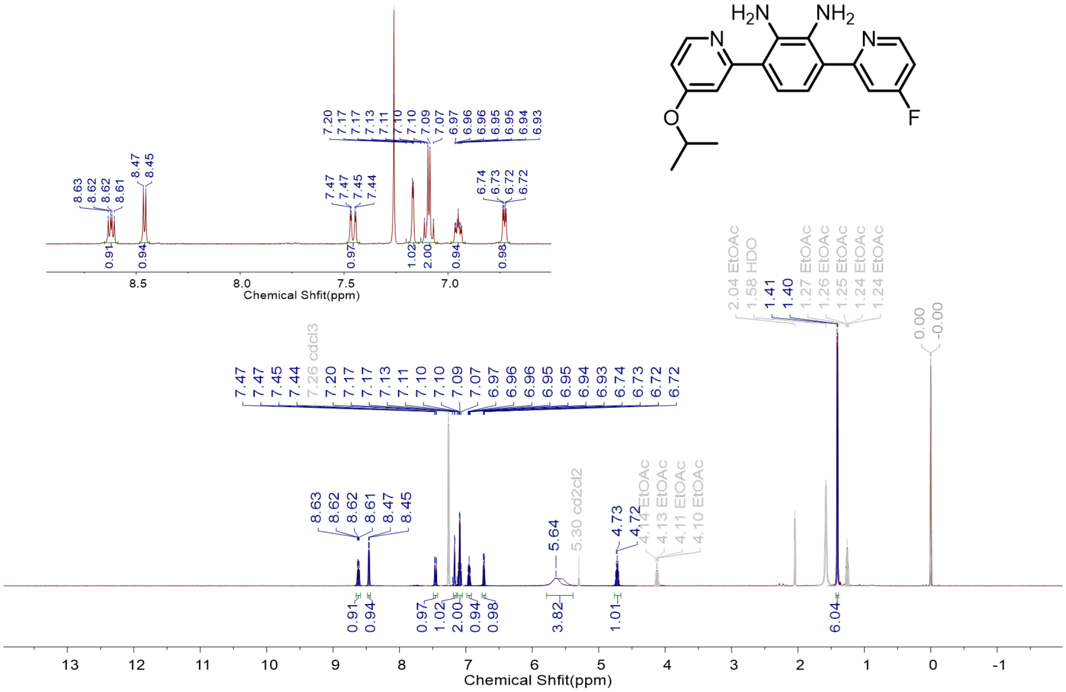

Figure S35. ^{1}H NMR (500 MHz) spectrum of **11** in CDCl$_3$ (T = 298 K).

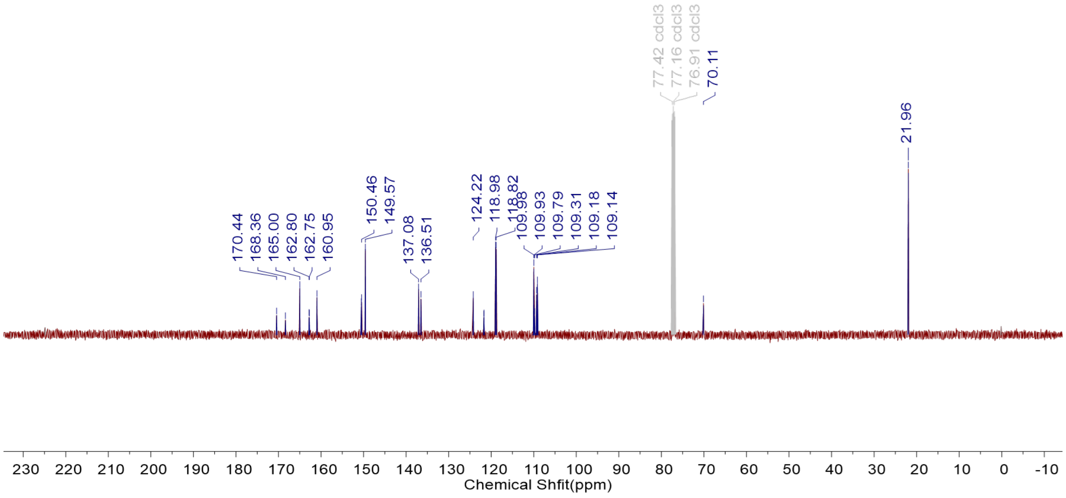

Figure S36. ^{13}C NMR (125 MHz) spectrum of **11** in CDCl$_3$ (T = 298 K).

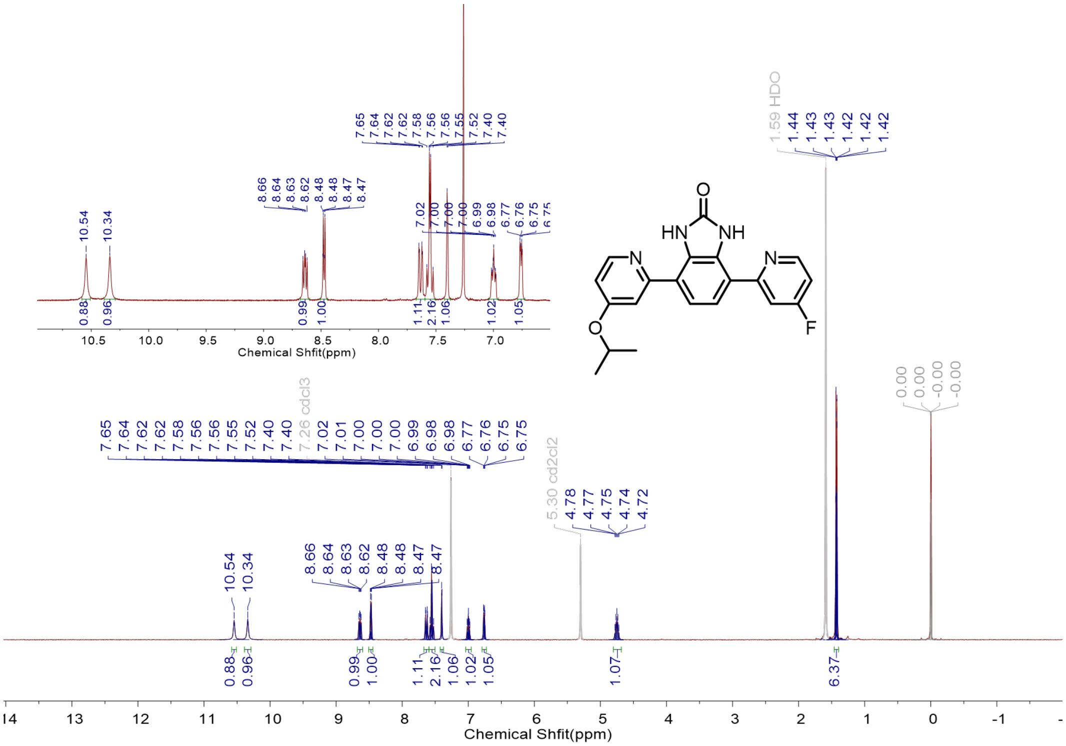

Figure S37. ^{1}H NMR (400 MHz) spectrum of **12** in CDCl$_3$ (T = 298 K).

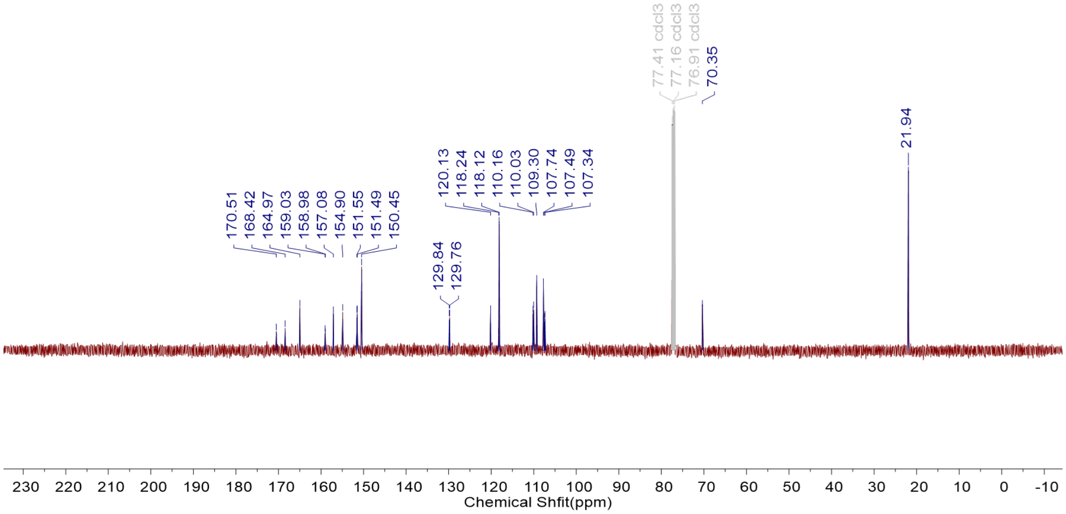

Figure S38. ^{13}C NMR (125 MHz) spectrum of **12** in CDCl$_3$ (T = 298 K).

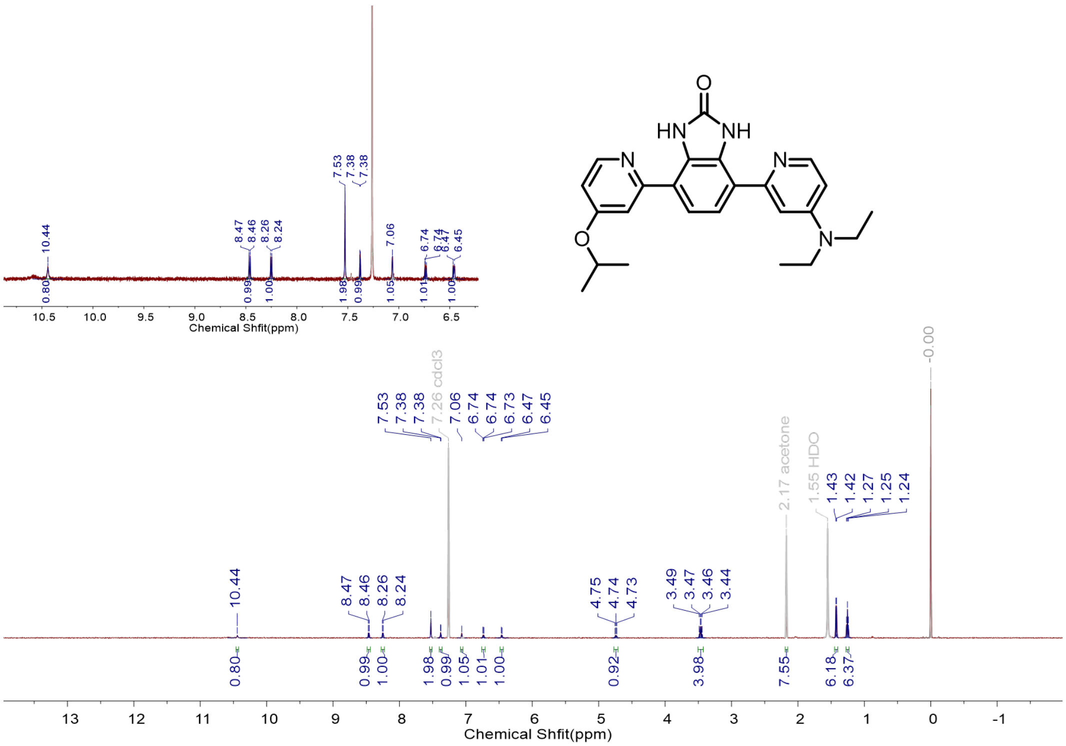

Figure S39. ^{1}H NMR (500 MHz) spectrum of **BZ-5** in $CDCl_3$ (T = 298 K).

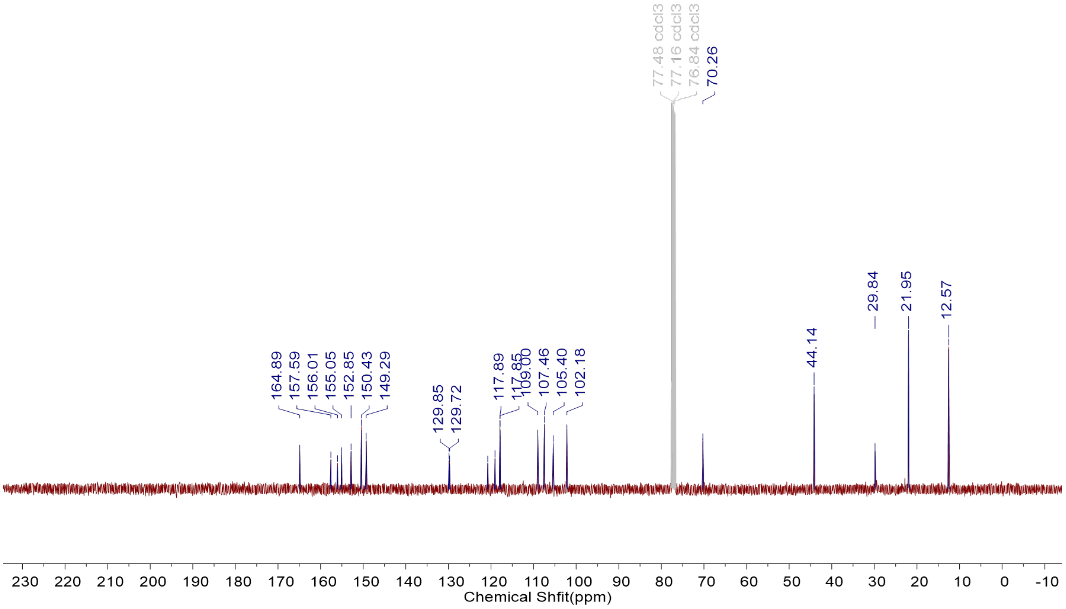

Figure S40. ^{13}C NMR (125 MHz) spectrum of **BZ-5** in $CDCl_3$ (T = 298 K).

Table S4. Cartesian coordinates of the optimized geometry of **BZ-1** at $\mathrm{S}_{1,\mathrm{N}^*}$.

E(TD-HF/TD-DFT) = −760.404690967 Hartree

Atom	x	y	z
C	0.000000	0.707656	0.420371
C	0.000000	1.493011	−0.776077
C	0.000000	0.713092	−1.941239
C	0.000000	−0.713092	−1.941239
C	0.000000	−1.493011	−0.776077
C	0.000000	−0.707656	0.420371
N	0.000000	−1.105607	1.723852
C	0.000000	0.000000	2.577855
N	0.000000	1.105607	1.723852
O	0.000000	0.000000	3.801454
C	0.000000	2.945909	−0.723641
C	0.000000	3.736776	−2.013485
O	0.000000	3.533421	0.390642
C	0.000000	−2.945909	−0.723641
O	0.000000	−3.533421	0.390642
C	0.000000	−3.736776	−2.013485
H	0.000000	1.204084	−2.908090
H	0.000000	−1.204084	−2.908090
H	0.000000	−2.083104	2.000945
H	0.000000	2.083104	2.000945
H	0.883254	3.510618	−2.623077
H	−0.883254	3.510618	−2.623077
H	0.000000	4.801265	−1.773761
H	0.883254	−3.510618	−2.623077
H	0.000000	−4.801265	−1.773761
H	−0.883254	−3.510618	−2.623077

Table S5. Cartesian coordinates of the optimized geometry of **BZ-1** at $\mathrm{S}_{1,\mathrm{T}^*}$.

E(TD-HF/TD-DFT) = −760.398736993 Hartree

Atom	x	y	z
C	0.723484	0.454511	−0.001244
C	1.537120	−0.721028	0.000278
C	0.821089	−1.920054	0.001456
C	−0.600584	−1.970064	−0.000410
C	−1.414249	−0.817938	−0.005412
C	−0.704753	0.414373	−0.003390
N	−1.232189	1.664961	−0.002578
C	−0.171446	2.538215	0.000092
N	1.039147	1.763322	0.000151
O	−0.173003	3.770551	0.002058
C	3.006157	−0.624831	0.000547
C	3.834447	−1.889743	0.001056
O	3.547820	0.491656	−0.000140
C	−2.844333	−0.834961	−0.006918
O	−3.511343	0.322566	0.004862
C	−3.718320	−2.036375	0.000972
H	1.350036	−2.865769	0.003966
H	−1.058121	−2.952482	0.004606
H	−2.868896	1.095695	0.007168
H	1.983545	2.129765	0.001946
H	3.617661	−2.499858	0.884821
H	3.617549	−2.500503	−0.882238
H	4.891139	−1.620224	0.000897
H	−4.258040	−2.104693	0.955845
H	−4.475351	−1.946463	−0.787409
H	−3.167689	−2.964267	−0.149019

Table S6. Cartesian coordinates of the optimized geometry of **BZ-2** at $\mathrm{S}_{1,\mathrm{N}^*}$.

E(TD-HF/TD-DFT) = −949.307139839 Hartree

Atom	x	y	z	Atom	x	y	z
C	0.000085	−0.711779	0.507431	C	0.000003	−5.730707	−0.427888
C	−0.000041	0.710996	−1.839634	N	0.000307	−3.543491	0.597670
C	0.000110	−1.509028	−0.683993	C	−0.000270	−3.759230	−1.819546
C	−0.000085	0.711779	0.507431	C	−0.000339	−5.138716	−1.707330
C	−0.000110	1.509028	−0.683993	C	0.000273	−4.878334	0.677398
C	0.000041	−0.710996	−1.839634	H	−0.000046	1.186713	−2.813659
N	−0.000169	1.104075	1.811488	H	0.000046	−1.186713	−2.813659
C	0.000000	0.000000	2.664345	H	0.000040	2.098565	2.049889
N	0.000169	−1.104075	1.811488	H	−0.000040	−2.098565	2.049889
O	0.000000	0.000000	3.890184	H	0.000030	6.806940	−0.296479
C	0.000000	2.956817	−0.646388	H	0.000414	3.301554	−2.802284
C	−0.000003	5.730707	−0.427888	H	−0.000568	5.289875	1.685161
C	0.000270	3.759230	−1.819546	H	−0.000030	−6.806940	−0.296479
N	−0.000307	3.543491	0.597670	H	−0.000414	−3.301554	−2.802284
C	−0.000273	4.878334	0.677398	H	0.000568	−5.289875	1.685161
C	0.000339	5.138716	−1.707330	H	−0.000567	−5.755812	−2.600803
C	0.000000	−2.956817	−0.646388	H	0.000567	5.755812	−2.600803

Table S7. Cartesian coordinates of the optimized geometry of **BZ-2** at $\mathrm{S}_{1,\mathrm{T}^*}$.

E(TD-HF/TD-DFT) = −949.326868619 Hartree

Atom	x	y	z	Atom	x	y	z
C	−0.754912	0.574002	0.034979	C	−5.732071	−0.506576	−0.051263
C	0.716970	−1.769469	0.091396	N	−3.579382	0.568638	0.040368
C	−1.489437	−0.629583	0.033837	C	−3.721162	−1.827708	−0.073883
C	0.695979	0.615195	0.063125	C	−5.111474	−1.756858	−0.097997
C	1.445272	−0.596356	0.096935	C	−4.917492	0.623780	0.015003
C	−0.705683	−1.787140	0.068867	H	1.241522	−2.718870	0.114200
N	1.148135	1.874196	0.048721	H	−1.184287	−2.758616	0.086814
C	0.012594	2.687351	0.019871	H	2.987448	−0.520153	−1.986782
N	−1.141680	1.870527	0.012971	H	−2.113550	2.160005	0.014044
O	−0.015822	3.915530	0.005021	H	6.797155	−0.592082	−0.255242
C	2.932558	−0.578706	0.100800	H	3.204373	−0.702922	2.186905
C	5.718670	−0.576995	−0.138765	H	5.340006	−0.473176	−2.270338
C	3.706087	−0.640476	1.227146	H	−6.811849	−0.406983	−0.068457
N	3.551739	−0.467484	−1.153497	H	−3.234930	−2.794505	−0.116857
C	4.944809	−0.510452	−1.264847	H	−5.353147	1.619252	0.049275
C	5.127845	−0.631043	1.153438	H	−5.701057	−2.666522	−0.154769
C	−2.973425	−0.638812	0.000257	H	5.732445	−0.691729	2.047699

Table S8. Cartesian coordinates of the optimized geometry of **BZ-3′** at $S_{0,\mathrm{min}}$.

E(B3LYP) = −1217.41195480 Hartree

Atom	x	y	z	Atom	x	y	z
C	−0.005574	0.706683	1.349012	C	0.604541	5.211535	−3.355391
C	0.000830	−0.696063	−1.020258	C	−0.604541	−5.211535	−3.355391
C	0.000000	1.461418	0.168817	C	−0.435766	−7.314203	−1.973040
C	0.005574	−0.706683	1.349012	H	0.009933	−1.197591	−1.980759
C	0.000000	−1.461418	0.168817	H	−0.009933	1.197591	−1.980759
C	−0.000830	0.696063	−1.020258	H	0.061123	−2.074118	2.945468
N	0.006784	−1.097430	2.679167	H	−0.061123	2.074118	2.945468
C	0.000000	0.000000	3.521890	H	−0.024632	−6.770104	0.479607
N	−0.006784	1.097430	2.679167	H	−0.355683	−3.178570	−1.916727
O	0.000000	0.000000	4.757003	H	0.267721	−5.318860	2.424459
C	−0.015139	−2.945714	0.190362	H	0.024632	6.770104	0.479607
C	−0.028541	−5.697426	0.339150	H	0.355683	3.178570	−1.916727
C	−0.201957	−3.690595	−0.978876	H	−0.267721	5.318860	2.424459
N	0.150206	−3.530607	1.403678	H	−0.488579	7.725577	−1.550217
C	0.136946	−4.871844	1.441068	H	1.278313	7.644225	−1.351356
C	−0.205729	−5.106306	−0.939429	H	0.564434	7.732366	−2.970620
C	0.015139	2.945714	0.190362	H	−0.228161	4.549895	−3.622619
C	0.028541	5.697426	0.339150	H	0.689212	5.973926	−4.128845
N	−0.150206	3.530607	1.403678	H	1.530018	4.620515	−3.353175
C	0.201957	3.690595	−0.978876	H	−0.689212	−5.973926	−4.128845
C	0.205729	5.106306	−0.939429	H	0.228161	−4.549895	−3.622619
C	−0.136946	4.871844	1.441068	H	−1.530018	−4.620515	−3.353175
N	−0.373878	−5.859016	−2.068185	H	−1.278313	−7.644225	−1.351356
N	0.373878	5.859016	−2.068185	H	0.488579	−7.725577	−1.550217
C	0.435766	7.314203	−1.973040	H	−0.564434	−7.732366	−2.970620

Table S9. Cartesian coordinates of the optimized geometry of **BZ-3′** at $\mathrm{S}_{1,\mathrm{N}^*}$.

E(TD-HF/TD-DFT) = −1217.28973664 Hartree

Atom	x	y	z	Atom	x	y	z
C	0.000340	0.711234	1.327626	C	−0.161673	5.328796	−3.363439
C	−0.000783	−0.710998	−1.018985	C	0.161673	−5.328796	−3.363439
C	0.000000	1.512362	0.136839	C	0.209509	−7.381900	−1.931151
C	−0.000340	−0.711234	1.327626	H	−0.003396	−1.185786	−1.993755
C	0.000000	−1.512362	0.136839	H	0.003396	1.185786	−1.993755
C	0.000783	0.710998	−1.018985	H	−0.003339	−2.100653	2.864114
N	−0.000928	−1.103472	2.632974	H	0.003339	2.100653	2.864114
C	0.000000	0.000000	3.485148	H	0.019952	−6.793283	0.544619
N	0.000928	1.103472	2.632974	H	0.039275	−3.258367	−1.962404
O	0.000000	0.000000	4.712897	H	−0.002807	−5.301663	2.481762
C	0.001007	−2.960996	0.176692	H	−0.019952	6.793283	0.544619
C	0.008819	−5.724313	0.382352	H	−0.039275	3.258367	−1.962404
C	0.017532	−3.748503	−1.000194	H	0.002807	5.301663	2.481762
N	−0.008971	−3.535959	1.425381	H	−1.199247	7.618758	−1.514623
C	−0.001962	−4.871816	1.481261	H	0.552440	7.842981	−1.294641
C	0.007819	−5.153231	−0.925133	H	−0.133684	7.837192	−2.918664
C	−0.001007	2.960996	0.176692	H	−1.137986	4.831773	−3.465876
C	−0.008819	5.724313	0.382352	H	−0.083017	6.097423	−4.132262
N	0.008971	3.535959	1.425381	H	0.622376	4.587437	−3.551949
C	−0.017532	3.748503	−1.000194	H	0.083017	−6.097423	−4.132262
C	−0.007819	5.153231	−0.925133	H	1.137986	−4.831773	−3.465876
C	0.001962	4.871816	1.481261	H	−0.622376	−4.587437	−3.551949
N	−0.008649	−5.943564	−2.052434	H	−0.552440	−7.842981	−1.294641
N	0.008649	5.943564	−2.052434	H	1.199247	−7.618758	−1.514623
C	−0.209509	7.381900	−1.931151	H	0.133684	−7.837192	−2.918664

Table S10. Cartesian coordinates of the optimized geometry of **BZ-3′** at $S_{1,\mathrm{TS1}}$.

E(TD-HF/TD-DFT) = −1217.28423438 Hartree

Atom	x	y	z	Atom	x	y	z
C	−0.698048	1.212525	0.003272	C	−5.469073	−3.324471	−0.054523
C	0.774956	−1.072861	−0.028011	C	5.455995	−3.283644	0.085085
C	−1.465037	−0.003451	0.003267	C	7.470355	−1.792710	0.107265
C	0.713427	1.280895	−0.010732	H	1.291771	−2.026157	−0.042917
C	1.538587	0.114580	−0.025583	H	−1.090314	−2.130085	−0.016733
C	−0.646808	−1.140007	−0.013692	H	1.971122	2.949010	−0.014859
N	1.009747	2.617987	−0.004885	H	−2.399694	2.322637	0.029497
C	−0.165178	3.380208	0.012085	H	6.807855	0.665615	−0.049293
N	−1.217266	2.462169	0.017118	H	3.346323	−1.939800	−0.012963
O	−0.239551	4.609925	0.020781	H	5.260817	2.557940	−0.050246
C	2.990961	0.188801	−0.037084	H	−6.722657	0.658809	0.049988
C	5.743803	0.472484	−0.051909	H	−3.314717	−2.038515	−0.003078
C	3.808335	−0.963776	−0.033304	H	−5.130415	2.523464	0.051778
N	3.525024	1.450799	−0.045973	H	−7.833751	−1.152225	0.749672
C	4.860021	1.545405	−0.050343	H	−7.717308	−1.302783	−1.020092
C	5.211882	−0.849698	−0.053648	H	−7.946952	−2.741724	−0.008968
C	−2.905510	0.073170	0.019551	H	−4.767801	−3.537714	0.760609
C	−5.663451	0.444486	0.046401	H	−6.285445	−4.043126	0.009765
N	−3.434844	1.356043	0.034970	H	−4.945560	−3.478042	−1.008977
C	−3.759499	−1.053730	0.016844	H	6.247057	−4.028934	0.003399
C	−5.157029	−0.898220	0.039717	H	4.719853	−3.491361	−0.699215
C	−4.765868	1.499223	0.045432	H	4.963297	−3.404496	1.061255
N	6.031804	−1.954259	−0.079531	H	7.898113	−1.149369	−0.668601
N	−6.007220	−1.974200	0.059118	H	7.950799	−2.768005	0.029696
C	−7.448223	−1.774581	−0.065163	H	7.715710	−1.362081	1.088750

Table S11. Cartesian coordinates of the optimized geometry of **BZ-3′** at S_{1,T^*}.

E(TD-HF/TD-DFT) = −1217.30540166 Hartree

Atom	x	y	z	Atom	x	y	z
C	0.702079	1.398831	−0.008587	C	5.253822	−3.388955	0.008539
C	−0.730065	−0.976202	−0.118758	C	−5.281793	−3.374862	0.110251
C	1.473512	0.182408	−0.053430	C	−7.366545	−1.970450	0.125721
C	−0.727094	1.374251	−0.017209	H	−1.208404	−1.947432	−0.173325
C	−1.512619	0.180696	−0.063827	H	1.169403	−1.947325	−0.168799
C	0.691037	−0.976027	−0.115431	H	−2.083319	2.956892	0.025195
N	−1.106108	2.679855	0.034017	H	3.011007	2.238455	0.001734
C	0.042872	3.493404	0.069122	H	−6.809750	0.510927	−0.023275
N	1.158838	2.678615	0.044782	H	−3.237063	−1.936283	0.004287
O	0.012653	4.733809	0.115022	H	−5.346126	2.468243	−0.059407
C	−2.980253	0.201340	−0.055102	H	6.809830	0.491541	0.014945
C	−5.738140	0.364546	−0.036423	H	3.215990	−1.952150	−0.038736
C	−3.741104	−0.981729	−0.026419	H	5.355618	2.474018	0.028116
N	−3.564296	1.433274	−0.067561	H	7.821807	−1.356473	−0.575434
C	−4.903899	1.473593	−0.055477	H	7.561817	−1.613367	1.167919
C	−5.151715	−0.931795	−0.028868	H	7.765360	−2.994017	0.071927
C	2.922267	0.166784	−0.041021	H	4.529603	−3.520472	−0.802925
C	5.738154	0.361686	−0.007977	H	6.010224	−4.166965	−0.089600
N	3.591036	1.393556	−0.020190	H	4.730354	−3.528964	0.966029
C	3.718575	−0.997142	−0.041865	H	−6.044477	−4.151466	0.059872
C	5.120296	−0.948173	−0.041099	H	−4.746952	−3.476053	1.065406
C	4.942621	1.472326	0.001676	H	−4.569672	−3.551518	−0.703817
N	−5.918106	−2.069528	−0.024450	H	−7.808708	−1.382847	−0.686343
N	5.894292	−2.082124	−0.078053	H	−7.650646	−1.509310	1.081877
C	7.333208	−1.998058	0.164296	H	−7.798014	−2.970263	0.085681

Table S12. Cartesian coordinates of the optimized geometry of **BZ-3′** at $S_{1,\mathrm{TS2}}$.

E(TD-HF/TD-DFT) = −1217.29106113 Hartree

Atom	x	y	z	Atom	x	y	z
C	0.700541	−1.306979	−0.008886	C	5.460632	3.276792	0.028376
C	−0.663197	1.146557	−0.027033	C	−5.499134	3.303218	−0.012463
C	1.501172	−0.113174	−0.024272	C	−7.472982	1.732194	0.014055
C	−0.720246	−1.216885	−0.002440	H	−1.112918	2.133996	−0.035791
C	−1.463683	0.003934	−0.010172	H	1.279161	2.031221	−0.050499
C	0.757722	1.080428	−0.034524	H	−2.480459	−2.251280	0.016963
N	−1.235448	−2.462992	0.012104	H	2.923543	−2.225604	−0.023130
C	−0.125922	−3.341824	0.014213	H	−6.723595	−0.689896	0.029651
N	1.065397	−2.616844	0.001381	H	−3.335131	2.033092	−0.015769
O	−0.223025	−4.584174	0.026155	H	−5.111026	−2.541777	0.035605
C	−2.917816	−0.065744	−0.000531	H	6.811366	−0.678777	−0.019677
C	−5.665992	−0.467120	0.020808	H	3.347088	1.948053	−0.016660
C	−3.771993	1.044886	−0.004660	H	5.256410	−2.583718	−0.017242
N	−3.432934	−1.342586	0.014094	H	7.700349	1.355496	1.118347
C	−4.764744	−1.512387	0.024235	H	7.906258	1.129106	−0.636398
C	−5.174818	0.877294	0.005962	H	7.948483	2.751114	0.051646
C	2.948782	−0.151271	−0.030522	H	4.946283	3.432627	0.988144
C	5.747574	−0.493266	−0.029639	H	6.257492	4.014329	−0.060880
N	3.549996	−1.410748	−0.031627	H	4.743629	3.457138	−0.780348
C	3.801218	0.969006	−0.029119	H	−6.328274	4.009291	−0.013348
C	5.199596	0.846672	−0.041966	H	−4.892511	3.486765	−0.908122
C	4.896120	−1.561528	−0.026045	H	−4.881300	3.502057	0.872220
N	−6.027284	1.942593	0.002473	H	−7.804206	1.172940	−0.869326
N	6.030508	1.938758	−0.073932	H	−7.973209	2.699623	0.009023
C	7.468398	1.776192	0.130210	H	−7.792236	1.188356	0.911359

Table S13. Cartesian coordinates of the optimized geometry of **BZ-3′** at $\mathrm{S}_{1,\mathrm{TT}^*}$.

E(TD-HF/TD-DFT) = −1217.30174925 Hartree

Atom	x	y	z	Atom	x	y	z
C	0.000000	0.719900	1.368709	C	0.000000	5.341930	−3.349439
C	0.000000	−0.706907	−1.022566	C	0.000000	−5.341930	−3.349439
C	0.000000	1.480567	0.148297	C	0.000000	−7.401416	−1.893686
C	0.000000	−0.719900	1.368709	H	0.000000	−1.191636	−1.992602
C	0.000000	−1.480567	0.148297	H	0.000000	1.191636	−1.992602
C	0.000000	0.706907	−1.022566	H	0.000000	−2.936364	2.207812
N	0.000000	−1.164165	2.645048	H	0.000000	2.936364	2.207812
C	0.000000	0.000000	3.429499	H	0.000000	−6.799386	0.567160
N	0.000000	1.164165	2.645048	H	0.000000	−3.265483	−1.965876
O	0.000000	0.000000	4.681929	H	0.000000	−5.289887	2.512725
C	0.000000	−2.929034	0.143526	H	0.000000	6.799386	0.567160
C	0.000000	−5.730986	0.409396	H	0.000000	3.265483	−1.965876
C	0.000000	−3.745238	−0.999312	H	0.000000	5.289887	2.512725
N	0.000000	−3.558159	1.378965	H	−0.890778	7.758630	−1.363387
C	0.000000	−4.905403	1.499531	H	0.890778	7.758630	−1.363387
C	0.000000	−5.150832	−0.911330	H	0.000000	7.843596	−2.888890
C	0.000000	2.929034	0.143526	H	−0.890276	4.719333	−3.504614
C	0.000000	5.730986	0.409396	H	0.000000	6.129448	−4.101451
N	0.000000	3.558159	1.378965	H	0.890276	4.719333	−3.504614
C	0.000000	3.745238	−0.999312	H	0.000000	−6.129448	−4.101451
C	0.000000	5.150832	−0.911330	H	0.890276	−4.719333	−3.504614
C	0.000000	4.905403	1.499531	H	−0.890276	−4.719333	−3.504614
N	0.000000	−5.945258	−2.020848	H	−0.890778	−7.758630	−1.363387
N	0.000000	5.945258	−2.020848	H	0.890778	−7.758630	−1.363387
C	0.000000	7.401416	−1.893686	H	0.000000	−7.843596	−2.888890

Table S14. Cartesian coordinates of the optimized geometry of the local minimum ($\tau = 31.5°$) of protonated **BZ-3′** in S_1 state.

E(TD-HF/TD-DFT) = −1217.74795827 Hartree

Atom	x	y	z
C	1.465815	0.079011	0.318884
C	−1.511094	0.100555	0.084832
C	0.733834	1.258656	0.069795
C	0.651527	−1.060988	0.420626
C	−0.765120	−1.053619	0.296798
C	−0.697681	1.273043	−0.033317
H	1.124764	−2.014660	0.628962
H	−1.263076	−2.010322	0.396829
N	−1.064646	2.542151	−0.306683
C	0.054729	3.379874	−0.407126
N	1.146279	2.543973	−0.164667
H	−2.060598	2.766033	−0.426828
H	2.105256	2.862151	−0.224779
C	−2.977618	0.173847	−0.027605
C	−5.704758	0.443323	−0.261501
N	−3.489859	1.411024	−0.271562
C	−3.782813	−0.961476	0.109721
C	−5.191105	−0.858114	−0.006015
C	−4.822329	1.507317	−0.380150
H	−6.765146	0.628641	−0.366656
H	−3.326413	−1.919822	0.307518
H	−5.211453	2.503554	−0.575768
C	2.911176	0.049800	0.457238
C	5.704569	0.246239	0.616782
C	3.713449	−0.994205	−0.013675
N	3.535579	1.194831	1.005124
C	4.914890	1.241428	1.091283
C	5.114771	−0.956518	0.054202
H	6.775652	0.374431	0.678743
H	3.209280	−1.824184	−0.489375
H	5.322327	2.133915	1.550789
O	0.068167	4.571485	−0.656978
N	−6.006198	−1.942853	0.121097
N	5.912743	−1.998558	−0.372376
C	−7.455015	−1.790231	0.006575
H	−7.927451	−2.761484	0.145383
H	−7.740618	−1.409669	−0.981540
H	−7.846909	−1.108116	0.770625
C	−5.438319	−3.262984	0.380009
H	−4.755818	−3.568537	−0.422596
H	−4.890988	−3.284652	1.330711
H	−6.243723	−3.993771	0.435473
C	5.285853	−3.135600	−1.035479
H	6.038364	−3.902486	−1.218735
H	4.512746	−3.572878	−0.396133
H	4.826864	−2.857945	−1.997110
C	7.327404	−1.756649	−0.656178
H	7.469964	−1.012706	−1.453016
H	7.787670	−2.692895	−0.971522
H	7.856756	−1.417664	0.238281
H	3.026938	1.720951	1.705854

Table S15. Cartesian coordinates of the optimized geometry of the global minimum ($\tau = 156.4°$) of protonated **BZ-3′** in S_1 state.

E(TD-HF/TD-DFT) = −1217.75602423 Hartree

Atom	x	y	z
C	−1.317467	−0.710163	−0.160881
C	1.545764	−0.043983	0.009557
C	−0.829434	0.623991	−0.212240
C	−0.284341	−1.698537	−0.038202
C	1.058183	−1.380858	0.049253
C	0.530979	0.938194	−0.123650
H	−0.559127	−2.743749	0.062513
H	1.752383	−2.202482	0.185553
N	0.633304	2.317343	−0.266473
C	−0.603639	2.893266	−0.470984
N	−1.496973	1.836715	−0.414687
H	1.513914	2.811324	−0.216898
H	−2.464174	1.951832	−0.673669
C	2.961276	0.293623	0.076886
C	5.646268	1.083729	0.213112
N	3.296248	1.613161	0.121570
C	3.978437	−0.688516	0.084130
C	5.324457	−0.294130	0.156713
C	4.581719	1.975478	0.194721
H	6.660337	1.444276	0.312460
H	3.725201	−1.732666	−0.019836
H	4.773499	3.043646	0.243392
C	−2.704935	−1.056130	−0.223155
C	−5.382473	−1.973292	−0.354664
C	−3.773942	−0.222367	0.179830
N	−3.048883	−2.337902	−0.659736
C	−4.338771	−2.766524	−0.723301
C	−5.114734	−0.634163	0.127047
H	−6.384226	−2.369714	−0.423848
H	−3.521859	0.723674	0.633174
H	−4.481495	−3.775193	−1.091470
O	−0.864400	4.087543	−0.658143
N	6.330409	−1.246894	0.184778
N	−6.139160	0.169857	0.532308
C	7.719813	−0.919421	−0.111746
H	8.176758	−1.778904	−0.604571
H	8.255682	−0.733240	0.826887
H	7.787442	−0.049734	−0.759990
C	6.049906	−2.639164	0.512289
H	5.278443	−2.704469	1.278081
H	5.718497	−3.166188	−0.391221
H	6.967489	−3.105029	0.869251
C	−5.856883	1.516216	1.018883
H	−6.794497	2.021221	1.245469
H	−5.247168	1.496011	1.931625
H	−5.327495	2.105102	0.260177
C	−7.516765	−0.321868	0.545420
H	−7.857025	−0.589544	−0.461362
H	−8.168760	0.464667	0.922055
H	−7.626179	−1.195529	1.198575
H	−2.327558	−2.933898	−1.039629